THE JOURNAL OF IMMUNOLOGY

Decoding the Regulation of Mast Cell Exocytosis by Networks of Rab GTPases

Nurit P. Azouz, Takahide Matsui, Mitsunori Fukuda and Ronit Sagi-Eisenberg

J Immunol published online 23 July 2012
http://www.jimmunol.org/content/early/2012/07/23/jimmunol.1200542

This information is current as of July 31, 2012.

Supplementary Material **http://www.jimmunol.org/content/suppl/2012/07/23/jimmunol.1200542.DC1.html**

Subscriptions Information about subscribing to *The Journal of Immunology* is online at: http://jimmunol.org/subscriptions

Permissions Submit copyright permission requests at: http://www.aai.org/ji/copyright.html

Email Alerts Receive free email-alerts when new articles cite this article. Sign up at: http://jimmunol.org/cgi/alerts/etoc

The Journal of Immunology is published twice each month by The American Association of Immunologists, Inc., 9650 Rockville Pike, Bethesda, MD 20814-3994.
Copyright © 2012 by The American Association of Immunologists, Inc. All rights reserved.
Print ISSN: 0022-1767 Online ISSN: 1550-6606.

Downloaded from http://jimmunol.org/ at Inst Superiore de Sanita-Roma on July 31, 2012

Published July 23, 2012, doi:10.4049/jimmunol.1200542

Decoding the Regulation of Mast Cell Exocytosis by Networks of Rab GTPases

Nurit P. Azouz,* Takahide Matsui,† Mitsunori Fukuda,† and Ronit Sagi-Eisenberg*

Exocytosis is a key event in mast cell functions. By this process, mast cells release inflammatory mediators, contained in secretory granules (SGs), which play important roles in immunity and wound healing but also provoke allergic and inflammatory responses. The mechanisms underlying mast cell exocytosis remained poorly understood. An essential step toward deciphering the mechanisms behind exocytosis is the identification of the cellular components that regulate this process. Because Rab GTPases regulate specific trafficking pathways, we screened 44 Rabs for their functional impacts on exocytosis triggered by the FcεRI or combination of Ca^{2+} ionophore and phorbol ester. Because exocytosis involves the continuous reorganization of the actin cytoskeleton, we also repeated our screen in the presence of cytochalasin D that inhibits actin polymerization. In this paper, we report on the identification of 30 Rabs as regulators of mast cell exocytosis, the involvement of 26 of which has heretofore not been recognized. Unexpectedly, these Rabs regulated exocytosis in a stimulus-dependent fashion, unless the actin skeleton was disrupted. Functional clustering of the identified Rabs suggested their classification as Rabs involved in SGs biogenesis or Rabs that control late steps of exocytosis. The latter could be further divided into Rabs that localize to the SGs and Rabs that regulate transport from the endocytic recycling compartment. Taken together, these findings unveil the Rab networks that control mast cell exocytosis and provide novel insights into their mechanisms of action. ***The Journal of Immunology*****, 2012, 189: 000–000.**

Regulated exocytosis is a central mechanism in mediating mast cell physiological functions in immunity and wound healing, as well as underlying this cell pathological functions in allergic and inflammatory reactions (1, 2). In doing so, externally triggered cells release a variety of preformed proinflammatory and immunomodulatory substances packaged in cytoplasmic secretory granules (SGs). The latter include vasoactive amines such as histamine and serotonin, proteases, such as chymase and tryptase, chemoattractants, and cytokines (3). Mast cell SGs also contain lysosomal hydrolases and lysosomal membrane proteins (3, 4) and are therefore considered secretory lysosomes, a property shared with SGs of other immune cells, including CTL, NK cells, and platelets (5). Once released, mast cell mediators affect multiple cells and organs, thus initiating an inflammatory response.

Given the pleiotropic functions of mast cells in health and disease (6), efforts are being undertaken to develop novel therapies that will specifically target mast cell activation (7). For this purpose, it is of great importance to elucidate the machineries and molecular mechanisms behind mast cell activation. Indeed, a large body of studies aimed at resolving the stimulus–secretion coupling mechanisms in activated mast cells. In particular, previous studies have delineated the signaling networks elicited by the FcεRI upon binding of the allergen to receptor bound allergen-specific IgE Abs (8–10). However, the mechanism underlying the secretory process remained poorly understood and challenging, because mast cells contain discrete types of SGs (11, 12) and release their contents by three exocytic mechanisms. The latter include kiss-and-run exocytosis that partially releases the SG cargo through a relative narrow and transient fusion pore; full exocytosis, when fusion of plasma membrane docked SGs, with the plasma membrane, allows complete expulsion of their contents, and third, compound exocytosis, the most extensive mode of cargo release, which involves homotypic fusion of SGs, allowing discharge of multiple granules, including those placed distal to the plasma membrane (13–15). In addition, the lysosomal nature of the mast cell SGs raises questions as to how are secretory lysosomes formed and how do they acquire their exocytosis competence. Consistent with the complexity of mast cell exocytosis, multiple SNARE proteins have been implicated in controlling this process (11, 16–18).

To gain insights into the mechanisms underlying mast cell exocytosis, we have undertaken work aimed at identifying the network of Rab GTPases that controls this process. More than 60 Rabs are expressed in mammals, regulating and coordinating discrete steps along the vesicular trafficking through their interactions with numerous effectors (19). Therefore, we reasoned that identification of the Rabs that regulate mast cell exocytosis should unveil the intermediate array of steps that culminate in this process. To do so, we applied a gain-of-function screen for Rabs that affect mast cell exocytosis triggered by the FcεRI or by a calcium ionophore and 12-*O*-tetradecanoylphorbol-13-acetate (TPA), considered to activate mast cells downstream of the receptor by elevating cytosolic Ca^{2+} and activating protein kinase C. In this paper, we identified Rab networks that regulate mast cell exocytosis in a stimulus and actin-dependent fashion.

*Department of Cell and Developmental Biology, Sackler Faculty of Medicine, Tel Aviv University, Tel Aviv 69978, Israel; and †Laboratory of Membrane Trafficking Mechanisms, Department of Developmental Biology and Neurosciences, Graduate School of Life Sciences, Tohoku University, Aobayama, Aoba-ku, Sendai, Miyagi 980-8578, Japan

Received for publication February 22, 2012. Accepted for publication June 21, 2012.

This work was supported by a grant from the Israel Science Foundation, founded by the Israel Academy for Sciences (to R.S.-E.), and partial support by a travel grant from the Constantiner Institute (to N.P.A.).

N.P.A. designed and performed the experiments, analyzed the data, and wrote the paper; T.M. constructed and validated the wt and CA Rab plasmids; M.F. supervised the construction and validation of the Rab plasmids, analyzed the data, discussed the results, and reviewed the paper at all stages; and R.S.-E. conceived and supervised the project, designed the experiments, analyzed the data, and wrote the paper.

Address correspondence and reprint requests to Dr. Ronit Sagi-Eisenberg, Department of Cell and Developmental Biology, Sackler Faculty of Medicine, Tel Aviv University, Tel Aviv 69978, Israel. E-mail address: histol3@post.tau.ac.il

The online version of this article contains supplemental material.

Abbreviations used in this article: CA, constitutively active; ERC, endocytic recycling compartment; ISG, immature secretory granule; KO, knockout; NPY, Neuropeptide Y; RNAi, RNA interference; SG, secretory granule; TPA, 12-*O*-tetradecanoylphorbol-13-acetate; wt, wild-type.

Copyright © 2012 by The American Association of Immunologists, Inc. 0022-1767/12/$16.00

Downloaded from http://jimmunol.org/ at Inst Superiore de Sanita-Roma on July 31, 2012

Materials and Methods

Materials

4-Bromo-calcium ionophore A23187, anti-DNP monoclonal IgE, DNP-HSA, cytochalasin D, and *p*-nitrophenyl-*N*-acetyl-β-D-glucosaminide were purchased from Sigma-Aldrich (St. Louis, MO). TPA was from Calbiochem (San Diego, CA). Hoechst was purchased from Invitrogen (Carlsbad, CA).

Abs used in this study

Anti-DNP monoclonal IgE and Hilyte Plus 647-conjugated goat anti-mouse IgG were from Anaspec (Fremont, CA); monoclonal anti-serotonin and monoclonal anti-tubulin were from Sigma-Aldrich. Mouse monoclonal anti-TGN38 was from BD Biosciences (Franklin Lakes, NJ); Cy2-conjugated donkey anti mouse IgG was from Jackson ImmunoResearch Laboratories (West Grove, PA); rabbit polyclonal anti-Rab42 IgG was produced using GST-Rab42.

Plasmids used in this study

pEGFP-wild-type (wt) Rab constructs have been described previously (20, 21). Constitutively active (CA) Rab mutants were prepared as previously described (22) and subcloned into the pEGFP-C1 or pEF-FLAG vectors. To construct the *Rab42* small interfering RNA expression vector, oligonucleotides containing the 19-base target site GTTAGTGCGAAGAATGACA were cloned into the pSilencer 2.1-U6 neo (Ambion, Austin, TX) as described previously (23). The nomenclature of the Rabs is according to Itoh et al. (22). pEGFP-Lifeact was from ibidi (Munich, Germany), and

Table I. Primers (5′→3′ direction)

Primer [C]	Primer [N]	Rab
GCACTGGTTTCCAAAAATGG	GCCATGGCATCATAGTTGTG	Rab1A
TGCTGTCGATCTTCAGGTTG	ATCGCTACGCCAGTGAGAAT	Rab1B
GAGATGCATTGGTAGCAGCA	TCAGCATTCCAATTCCAACA	Rab2A
AGGCTGTCTTGGCTGATGTT	TTTGGAGCACGTATGGTCAA	Rab2B
GGCCTCAAAGAACTCAAAGC	GCAGAAGGAGTCCTCAGACC	Rab3A
AGGGGTCTGTGTCCATTGAG	CTTCCTTTTCCGCTATGCTG	Rab3B
TGTATCTTTCCTGGCCTGCT	ACAAGATGCCAGGTTTGGTC	Rab3C
AGTAGGCCGTGGTGATTGTC	GCTATGCCGATGACTCCTTC	Rab3D
GTGCACTTGGAGCCTGTGTA	ATGTTCCTGGAAACCAGTGC	Rab4A
GGCGAAGAGATATGTCACCATAC	CAGCCGGGAGACATACAACT	Rab4B
CTCGTCCTCTGGCTGAGTTT	CTTCAAAGGCAAGCAAGTCC	Rab5A
CACTGGCTCTTGTTCTGCTG	GCCAGCAAAATATGCCAGTT	Rab5B
TGAAACTCCACGGCTCTCTT	CAAGCAGCCATTGTGGTCTA	Rab5C
GCAGCAGAGTCACGGATGTA	GAATCCGCTGAGGAAATTCA	Rab6A
TGTCAATCATCCCTTCTTTGC	ACAACACCTACCAGGCAACC	Rab6B
TCTTTGTGGCCACTTGTCTG	TACCATGCAGATCTGGGACA	Rab7
GTCCTCTTCTGCTGCTCCAC	GAGAAAAGCTGGCACTCGAC	Rab8A
AGCAGAGAACACCGGAAGAA	TGGAGACAAGTGCAAAATCG	Rab8B
TCGGTGCAGATTGACTGTGT	TGTGATTTTGGGCAACAAGA	Rab9A
CAGCTTCTTCAAAGGCCACT	GGAGGTAGATGGACGCTTTG	Rab9B
TTTCGGAGGATGTCTTCAGC	CTGCTTTTCAAGCTGCTCCT	Rab10
TTGGCTTGTTCTCAGTGGTG	TTGCAACAAGAAGCATCCAG	Rab11A
GATGTCCACCACATTGTTGC	CTGTCACGCTTCACCAGAAA	Rab11B
CTGCTGTGCAAACTTTTCTCC	TCAAGCTGCAGGTCATCATC	Rab12
TGTCTTGAGCAAGATGTCACG	AGCCTACGACCACCTCTTCA	Rab13
AGACTCGGCAGCATTCAGAT	GGCTGATTGTCCTCACACAA	Rab14
AGCACCAGCAGGTCTTTGAA	TCCACTCCTCGCATATCTCC	Rab15
CAGCATCACCACCACCTCT	GCGTCTGCCACCTCTACTTC	Rab17
TCGACTTCACGGTTTTCCTT	ATCCAGAACTTGCAGCAACA	Rab18
AAGAACTGGGCTGGAATCCT	ATGCTGATCGGGAACAAATC	Rab19
TGTTGGCTGTTTCTGTCAGG	GGGACATGAACGTGGGTAAA	Rab20
CTCCAGCTCAAACAGGCTCT	CGCCTTCTACCTGAAGCAGT	Rab20-inner primer
TGCCTCTCCTTTTCCAAGTC	AACGACAAGCACATCACCAC	Rab21
GGCTGTCTTCGGAGTTTGAA	CAGGGAACAAGTGCGATCTTA	Rab22A
TTGTAGGTGTTTCTCAGCCAAA	CAGGCTTGTGTGCTTGTGTT	Rab23
AGCTTTAGCACCCCGGTAAT	ATTTGGGACACAGCAGGTTC	Rab24
CCTGGCTGAGGTCACTTTTG	GCAAGACCAATCTGCTGTCC	Rab25
TCTCCCCATCTTCCCTCTTT	GCTGCTCTACGACATCACCA	Rab26
ATCCGCTTCATGATCAGGTC	TTCCTGCTTCTGTTCGACCT	Rab27A
CCACTGACTTCTCTACATTCTGTCC	ATTAAACTCCTGGCCCTTGG	Rab27B
TGCCTTCACCACTCTCTGTG	TTTTGCCAGGAAAATGGTTT	Rab28
AGCCCGTAAAACCGTTCTCT	GCGTTTCACATCCATGACAC	Rab29/Rab7L
AGCTGATGCTTTTCCCCTCT	GTGGGCAACAAGATTGACCT	Rab30
CAAGGTATGAAATGAATCCTGCT	ACGGGAGCTCAAAGTGTGTC	Rab31
ATCCTTGGCAGAGGTTTCAA	AGACCCGAGAGCACCTCTTT	Rab32
TTGGAGGGTACCTGGATCTG	GATGGACCAGTACGTGCAGA	Rab33A
TTGGGGTTTTTAGCAGAGGTC	AAGACGTGCCTGACTTACCG	Rab33B
TAATCTCTTGGGCCACCTTG	ACAAGGCTACCATCGGAGTG	Rab34
TGAGCTTCACCACATCGTTC	CTTCAAGCTGCTCATCATCG	Rab35
GCTGGGCCTCTTCTCTAGGT	CATCACCAGCTTCCCTAAGTG	Rab36
AGTCTCGGATCTGGAAGCTG	CCATGCTTATTACCGAGATGC	Rab37
GCTTCACAATGTCCGGTTCT	AGACCAGCCACATTTGAAGC	Rab38
CTTTTAACCCCTTCCCATCC	GTCGGCGTGGACTTCTTCT	Rab39A
GTTGGCAGTGAGGGAGTAGG	AAACTGCAGCTTTGGGACAC	Rab40B
TCTTAAGGCTGTTGCCCTTG	CTGCTCAAGTTCCTGCTGGT	Rab40C
GTCTCGATGGCACAGAGGAT	ACCATGAAGACGCTGGAGAT	Rab41
CCTGGAGAGAGCTTGATGGA	TGAATCCCCGAAAGAAAGTG	Rab42/Rab7B
CCCAGAGAGGCAGCAAGTT	GTGACCTGAACACCGATG	Rab43

Downloaded from http://jimmunol.org/ at Inst Superiore de Sanita-Roma on July 31, 2012

NPY-mRFP was a gift from U. Ashery (Tel Aviv University, Tel Aviv, Israel).

Cell Culture

Rat basophilic leukemia-2H3 cells (RBL-2H3, in this paper referred to as RBL) were maintained in adherent cultures in DMEM supplemented with 10% FBS in a humidified atmosphere of 5% CO_2 at 37˚C.

RNA isolation, reverse transcription, and PCR amplification

Total RNA was isolated using the RNeasy Mini kit (Qiagen, Hilden, Germany). Two-step RT-PCR was performed using reverse transcriptase (Promega, Madison, WI) with random decamers and Taq DNA Polymerase (Invitrogen). PCR was performed using the Readymix solution (Thermo Fisher Scientific, Waltham, MA). The primers used in this study are listed in Table I.

Transfection of RBL cells

Transient transfection of RBL cells was performed as described previously (16). Briefly, 1.5×10^7 RBL cells were transfected with 20 μg NPY-mRFP cDNA and 30 μg of either pEGFP or pEGFP-Rab or pEF-Flag-Rab cDNAs by electroporation at 300 V and 1500 μF. The cells were immediately replated in tissue culture dishes containing growth medium.

Flow cytometry

RBL cells were transiently transfected with GFP-wt or GFP-CA Rab27A or Rab42 cDNAs. Next day, cells were washed three times in ice-cold PBS and then incubated on ice for 1 h. Cells were then analyzed using a FACSort flow cytometer (BD Biosciences), and the average expression of the GFP-fused proteins was determined using the FCSexpress software.

Activation of RBL cells

Cells were seeded in 24-well plates (5×10^5 cells/well) and incubated overnight with 1 μg/ml mouse anti-DNP specific monoclonal IgE. Following three washes in Tyrode buffer (10 mM HEPES [pH 7.4], 130 mM NaCl, 5 mM KCl, 1.4 mM $CaCl_2$, 1 mM $MgCl_2$, 5.6 mM glucose, and 0.1% BSA), cells were stimulated in same buffer for 30 min at 37˚C with the desired stimuli (i.e., a combination of 4-bromo-calcium ionophore A23187 [Ion] and the phorbol ester [TPA], or DNP-HSA [Ag]).

Secretion of β-hexosaminidase

Activity of the SG-associated enzyme β-hexosaminidase was determined as described previously (16). Briefly, 20-μl aliquots of supernatants and cell lysates were incubated for 90 min at 37˚C with 50 μl substrate solution consisting of 1.3 mg/ml *p*-nitrophenyl-*N*-acetyl- β-D-glucosaminide in 0.1 M citrate (pH 4.5). Reactions were stopped by the addition of 150 μl 0.2 M glycine (pH 10.7). OD was measured at 405 nm. Results were expressed as percentage of total β-hexosaminidase activity present in the cells. For measurement of serotonin release, cells were incubated overnight with 2 μCi [^{3}H]5-hydroxytryptamine (GE Healthcare, Little Chalfont, Buckinghamshire, U.K.), washed, and stimulated as above. Aliquots from the supernatants and cell lysates were taken for measurement of radioactivity.

Secretion of NPY-mRFP

The fluorescence of cell supernatants and cell lysates (200 μl) was measured by an "INFINITE 200" (Tecan, Männedorf, Switzerland) fluorescence plate reader, using a 590-, 20-nm bandwidth, excitation filter and 635-, 35-nm bandwidth emission filter. Autofluorescence of nontransfected RBL cells was set as reference. The amount of secretion is presented as the percentage of secretion from control cells.

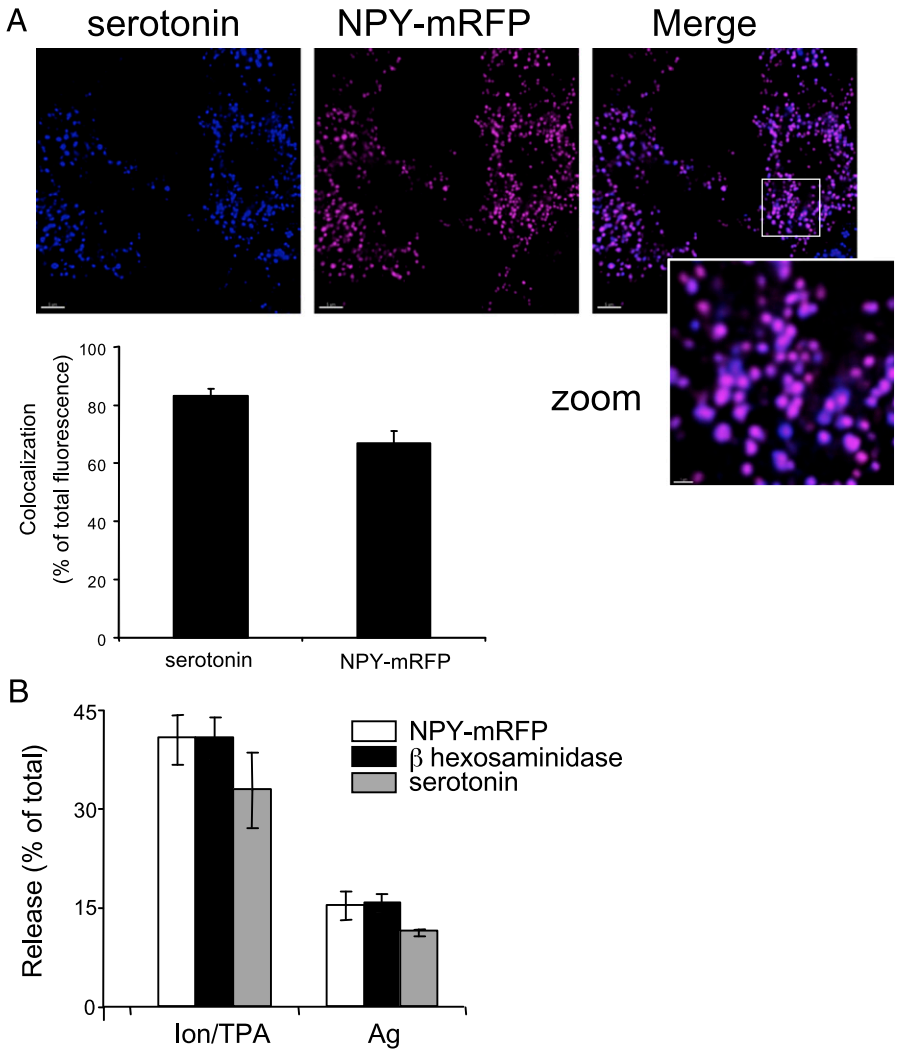

FIGURE 1. NPY-mRFP is targeted to SGs and released in a regulated fashion. (**A**) RBL cells, transiently transfected with NPY-mRFP cDNA, were immunostained using mAbs directed against serotonin, followed by Hilyte Plus 647-conjugated anti-mouse IgG. Images were captured and analyzed by confocal microscopy as described under *Materials and Methods*. A representative image is shown. Scale bar, 5 μm. The *inset* is an enlargement of the boxed area. Scale bar, 1 μm. Colocalization of endogenous serotonin with NPY-mRFP was quantified by the Zeiss LSM510 software. Data are means ± SEM from six coverslips from three independent experiments. (**B**) Release of NPY-mRFP, endogenous β-hexosaminidase, and serotonin from cells triggered for 30 min with 5 μM Ca^{2+} ionophore and 50 nM TPA (Ion/TPA) or 50 ng/ml DNP-HSA (Ag) was determined and is presented as percentage of total. Data are the means ± SEM from three independent experiments.

Downloaded from http://jimmunol.org/ at Inst Superiore de Sanita-Roma on July 31, 2012

Immunostaining and confocal analyses

RBL cells (4×10^5 cells/ml) were grown on 12-mm round glass coverslips, washed three times with PBS, and fixed for 30 min at room temperature with 4% paraformaldehyde in PBS. Cells were then permeabilized for 30 min at room temperature with 0.1% Triton X-100, 5% FBS, and 2% BSA diluted in PBS. Cells were subsequently incubated for 1 h at room temperature with the primary Abs, followed by three washes and 1-h incubation with the appropriate secondary Abs. After washing, cells were mounted (Golden Bridge Life Science, Mukilteo City, WA) and analyzed by a Zeiss 510 laser confocal microscope (Zeiss, Oberkochen, Germany) or Leica microscope (Leica, Wetzlar, Germany), using a ×63 oil/1.4 NA objective.

Time-lapse microscopy of living cells

RBL cells were seeded at 2×10^5 cells/chamber in an 8-well chamber borosilicate coverglass system (Thermo Fisher Scientific Waltham, MA). Images were acquired after 24 h by a Zeiss 510 laser confocal microscope, equipped with a heated chamber (37°C) and CO_2 controller (4.8%) and a "C-Apochromat" ×63/1.2 W Corr objective.

Statistical analysis

Data are expressed as means ± SEM. *p* Values were determined by unpaired two-tailed Student *t* test.

Results

The expression profile of Rab GTPases in RBL cells

We first analyzed the expression profiles of endogenous Rab GTPases in RBL cells, our mast cells model. To do so, we designed primers based on the rat Rabs sequences described so far (Table I). RT-PCR using these primers and RBL cell cDNA as template has yielded 54 products, excluding Rab20, Rab26, and Rab41. A second round of nested PCR amplified Rab20 and Rab26, therefore indicating that RBL cells express endogenously 57 of the 58 rat Rabs, whereby Rab20 and Rab26 are of lower abundance and Rab41 is either not expressed or is present in minute amounts (Supplemental Table I). Strikingly, the list of endogenously expressed Rabs included all corresponding Rab isoforms as well as Rabs considered epithelial specific and normally implicated in controlling polarized transport (i.e., Rab13, Rab17, Rab20, and Rab25) (24–27).

Development of a quantitative screening methodology

Next, a quantitative screening methodology was sought to sift out Rab functional redundancy (19) as well as compensate for the low

Downloaded from http://jimmunol.org/ at Inst Superiore de Sanita-Roma on July 31, 2012

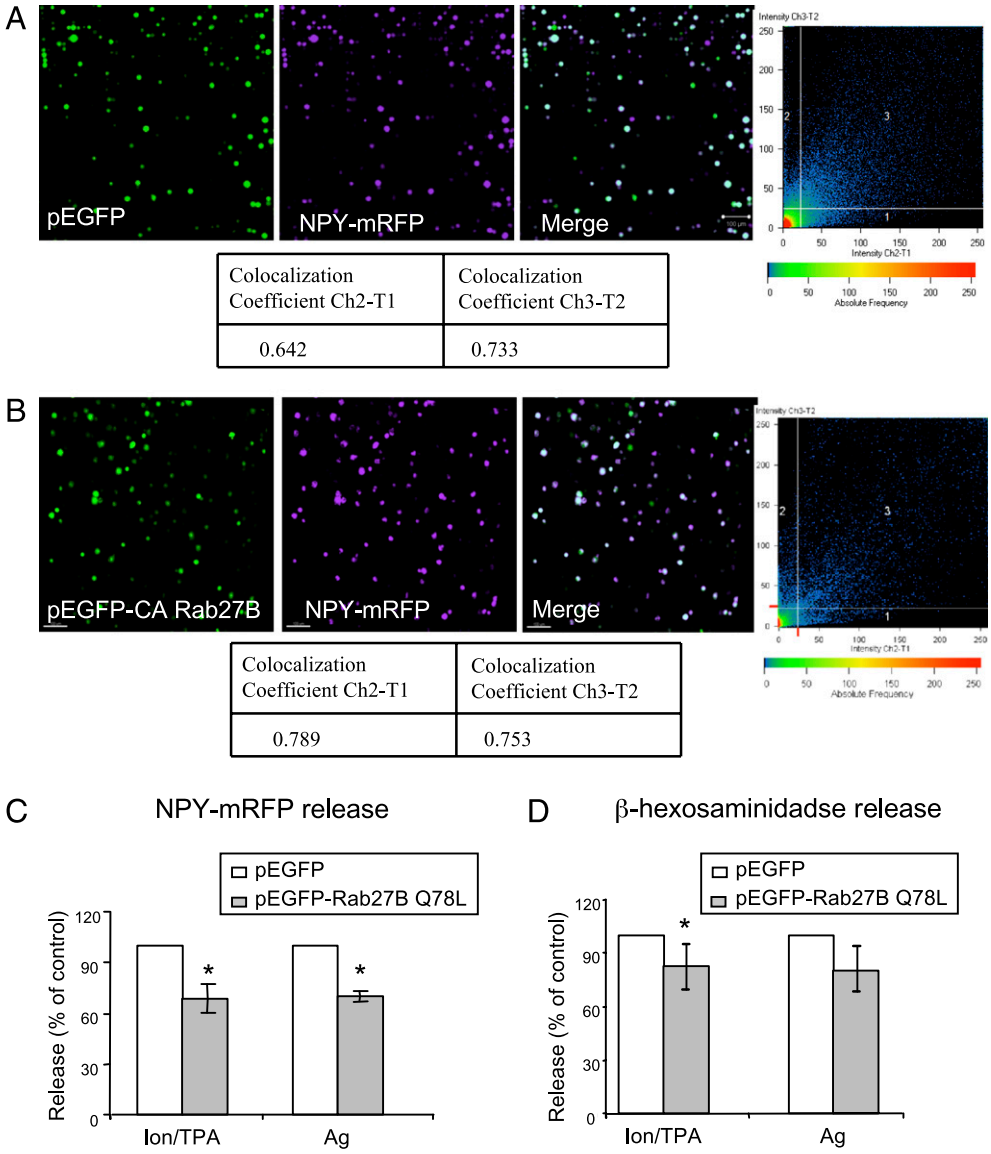

FIGURE 2. NPY-mRFP release is affected by CA Rab27B expression. Cells transiently cotransfected with NPY-mRFP and either pEGFP (**A**) or pEGFP-CA Rab27B (**B**) cDNAs were fixed and coexpression quantified by the Zeiss LSM510 software. Scale bar, 100 μm. Release of NPY-mRFP (**C**) or of endogenous β-hexosaminidase (**D**) in response to Ion/TPA or Ag was measured and is presented as percentage of release from control pEGFP-expressing cells. The data are means ± SEM of 11 independent experiments. *p = 0.014 (Ion/TPA); *p = 0.026 (Ag).

transfectability of RBL cells; the former is likely to hinder functional screening by Rab-specific small interfering RNAs, whereas the latter might impede interpretation of results based on average secretion readouts of the endogenous mediators.

Rab function involves cycling between inactive, GDP-bound, to active, GTP-bound conformations. Single residue mutations in Rabs can trap the protein in either a GDP-bound conformation, generating a constitutively negative mutant, or a constitutively active conformation, which remains GTP bound (CA mutant). In their active GTP-bound forms, Rabs bind their numerous effectors and are likely to scavenge effectors shared by functionally redundant Rabs. Therefore, such mutants are more likely to reveal their downstream functions, compared with the alternative approach of identifying their targeting events by specific Rabs RNA interference (RNAi). Indeed, CA Rab mutants were successfully used to identify Rab effectors and cellular functions (28–31). Furthermore, expression of GFP fusions of each of these proteins allows spatiotemporal correlations of their functional impacts that should be useful for decoding their underlying mechanisms. Finally, coexpression of a Rab mutant with a reporter for exocytosis enables exclusive monitoring of the Rab-expressing cells, thereby overcoming the low transfectability barrier. Therefore, we have carried out a gain-of-function screen combined with coexpression of a reporter for exocytosis.

For a reporter of exocytosis, we chose Neuropeptide Y fused to monomeric RFP (NPY-mRFP), previously shown to recapitulate the behavior of endogenous SG markers in other systems (32). Moreover, because mRFP fluorescence is pH insensitive, expression of NPY-mRFP not only allows quantitative assessment of exocytosis by using 96-well plates and a fluorescence plate reader but also it permits visualization of the acidic SGs. Indeed, transient transfection of RBL cells with NPY-mRFP resulted in its expression and targeting to vesicular structures, most of which also stained positive for the endogenous SG marker serotonin (Fig. 1A). Specifically, 83% of serotonin containing granules also contained NPY-mRFP, whereas 67% of NPY-mRFP–containing vesicles also contained serotonin (Fig. 1A). Therefore, this distribution pattern is consistent with delivery of NPY-mRFP to pre-existing serotonin containing SGs.

NPY-mRFP was also released in a regulated fashion alongside the endogenous mediators β-hexosaminidase and serotonin, in response to either an FcεRI-dependent trigger (by Ag) or by the combination of a Ca^{2+} ionophore and TPA (Ion/TPA) (Fig. 1B). Therefore, these results supported the use of NPY-mRFP as a genuine reporter for mast cell-regulated exocytosis.

Next, we established conditions for significant coexpression of NPY-mRFP and the cotransfected plasmid. We tested pEGFP (Fig. 2A) or pEGFP-Rab27B Q78L that encodes a GFP-CA Rab27B mutant (Fig. 2B). Moreover, because the involvement of Rab27B in regulating mast cell exocytosis is well established (33–35), the CA mutant of this Rab also served to validate our experimental setting. Expression of CA Rab27B significantly reduced NPY-mRFP release compared with release from control GFP-expressing cells (Fig. 2C). Therefore, CA Rab27B recapitulated the functional impact of Rab27B knockout (KO) on histamine release, previously recorded in mast cells derived from KO mice (34). In this context, it is important to note that although constitutively active mutants of Rabs that positively regulate exocytosis may enhance the secretory process, such mutants might display inhibitory impacts, stemming from over stimulation of their regulated intermediate steps. The latter may perturb cellular homeostasis or freeze the exocytic process at the exaggerated intermediate step, eventually interfering with propagation of the secretory process.

Only minor inhibition of β-hexosaminidase release was recorded under these conditions (Fig. 2D), supporting the need for reporter-based assays in functional genomics analyses of mast cell exocytosis.

Functional impacts of Rab GTPases and their phenotypic correlates

Forty-four CA Rab mutants were coexpressed with NPY-mRFP in RBL cells, where coexpression with GFP served as control. NPY-mRFP release in response to either FcεRI-clustering, induced by treating DNP-specific IgE-bound cells with DNP-HSA (Ag) or Ion/TPA, was measured and quantified. Relative release responses are presented in Table II and color-coded in Fig. 3.

At first glance, we could categorize the analyzed Rabs into four groups: the largest group included 23 Rabs, whose CA mutants expression had no effect on exocytosis; the second group comprised 11 CA Rabs that inhibited exocytosis triggered by both stimuli

Table II. Expression of CA Rab mutants affects NPY-mRFP release from triggered RBL cells

CA Mutant	Ion/TPA	±SEM	Ag	±SEM	*n*
GFP	100	0	100	0	
Rab1A	82	3.07	83	9.52	3
Rab2A	49	4.75	146	39.49	6
Rab3A	67	14.72	88	29.39	4
Rab4A	89	6.75	64	5.91	3
Rab5A	91	3.44	92	4.29	8
Rab6A	139	7.17	109	2.9	3
Rab7	65	3.68	70	4.09	5
Rab8A	71	3.51	76	4.9	22
Rab8B	92	2.67	112	6.6	3
Rab9A	67	12.86	76	5.18	5
Rab10	73	5.87	75	6.17	4
Rab11A	76	9.32	72	10.44	5
Rab11B	85	9.09	82	1.06	3
Rab12	67	4.6	69	4.56	10
Rab13	106	1.76	168	43.78	4
Rab14	61	7.37	83	13.57	4
Rab15	103	10.47	102	8.27	3
Rab17	80	4.64	96	9.07	3
Rab18	88	6.78	117	11.04	3
Rab19	59	10.38	69	5.34	3
Rab20	79	5.16	64	2.67	8
Rab21	90	7.6	113	19.91	3
Rab22A	78	3.69	72	2.35	3
Rab23	84	5.49	88	8.71	3
Rab24	103	11.92	89	4.8	3
Rab26	85	13.47	120	18.92	3
Rab27A	82	8.55	89	12.97	3
Rab27B	69	10.05	64	4.6	11
Rab28	100	4.14	118	2.27	3
Rab29	93	4.25	97	13.93	3
Rab30	127	17.51	93	6.07	3
Rab32	89	2.39	96	12.25	3
Rab33A	90	4.14	88	8.82	3
Rab34	112	9.07	126	11.49	3
Rab35	75	8.28	91	7.49	3
Rab36	95	8.86	106	23.54	3
Rab37	106	13.07	161	18.53	3
Rab38	102	1.62	66	9.03	3
Rab39A	71	7.25	84	3.46	3
Rab40	88	13.56	92	2.4	3
Rab41	90	4.38	80	6.51	3
Rab42	80	11.76	92	6.49	3
Rab43	68	9.1	67	14.89	4

RBL cells were cotransfected with NPY-mRFP and either pEGFP or pEGFP-CA Rab mutant cDNAs and grown for 24 h in the presence of DNP-specific IgE (1 μg/ml). Cells were subsequently left untreated or stimulated for 30 min with 50 ng/ml DNP-HSA (Ag) or 5 μM Ca^{2+} ionophore and 50 nM TPA (Ion/TPA). Release of NPYmRFP was determined as described in *Materials and Methods* and compared with release from control, pEGFP-expressing cells (set as 100%). Data are means ± SEM (for $n \geq 3$).

Downloaded from http://jimmunol.org/ at Inst Superiore de Sanita-Roma on July 31, 2012

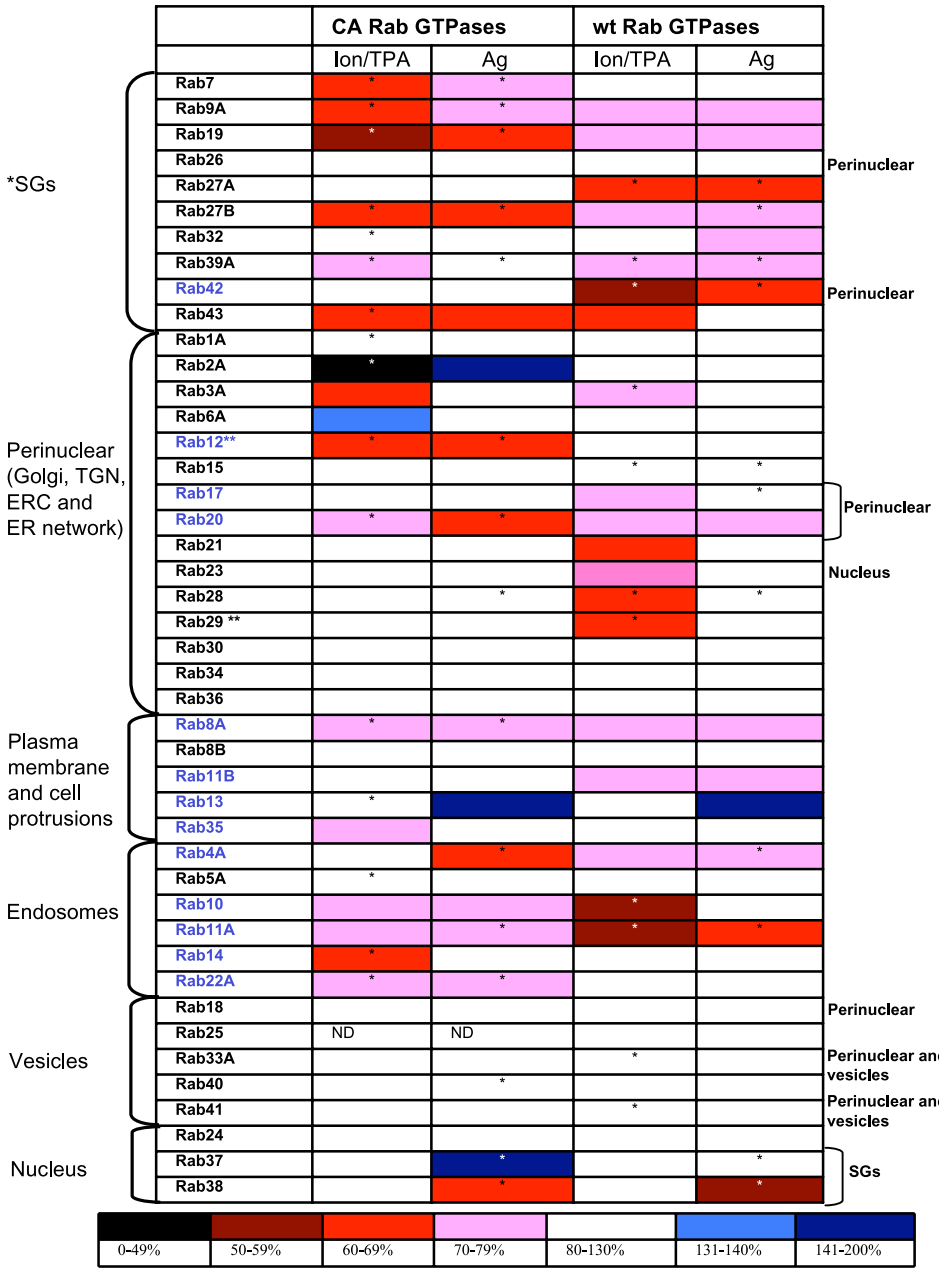

FIGURE 3. Triggered exocytosis is affected by expression of CA mutants or wt Rabs. RBL cells were cotransfected with NPY-mRFP and each of the indicated pEGFP-CA mutant or wt Rabs and grown for 24 h in the presence of DNP-specific IgE (1 μg/ml). Cells were subsequently left untreated or stimulated for 30 min with Ion/TPA or Ag. NPY-mRFP release was measured and compared with release from cells coexpressing NPY-mRFP and pEGFP. Release of NPY-mRFP (percentage of control) is presented in Tables II and III. Rabs were grouped according to their cellular location and colored according to the indicated color code, reflecting their inhibitory efficacy. The cellular location of CA Rab mutants (shown in Supplemental Fig. 1) is indicated. The localization of wt Rabs is indicated on the *right*. In blue are Rabs, whose function is associated with endocytic recycling. *Rabs were defined as SG localized when their extent of colocaization with NPY-mRFP, based on quantification of at least 30 cells by the Zeiss LSM510 software, exceeded 60%. **Colocalization of CA Rab12 and CA Rab29 with NPY-mRFP resulted from these Rabs induced alteration of the subcellular distribution of NPY-mRFP. $*p < 0.05$.

(Fig. 3). Surprisingly, two groups of Rabs affected exclusively either FcεRI-mediated exocytosis or exocytosis stimulated by Ion/TPA (Fig. 3).

To gain insights into the pathways that are possibly affected by the expression of active Rab mutants, we analyzed the Rabs identified in our screen according to their known functions in other cellular systems and their gain-of-function phenotypes. Hoechst staining allowed the visualization of cell nuclei to exclude defects that might originate from cell damage. In two cases, expression of CA mutants that modulated exocytosis stimulated by any of the applied triggers was also linked with altered cell morphology. Consistent with previous reports (36), CA Rab8A induced formation of membrane protrusions (Fig. 4A). SGs seemed to be captured in these protrusions (Fig. 4A), possibly accounting for their reduced capacity to degranulate. Second, CA Rab12 clearly promoted perinuclear clustering of the SGs (Fig. 4B). No clear phenotype was recorded for the remaining Rabs (Supplemental Fig. 1A). However, analysis of their cellular localization indicated that this group included Rabs that localized to the SGs in resting or activated cells (i.e., Rab27B, Rab19, Rab43, Rab7, and Rab9A; Supplemental Fig. 1A). Interestingly, members of this functional group, which did not localize to the SGs (i.e., Rab8A, Rab10, Rab11A, Rab12, Rab20, and Rab22A), are all implicated in regulating transport from the endocytic recycling compartment (ERC) (26, 29, 36–39), a discrete pericentriolar endosomal organelle, implicated in slow endocytic recycling (29).

CA mutants that exclusively affected either Ag or Ion/TPA-induced release included Rabs that stimulated release (i.e., CA Rab6A that stimulated Ion/TPA-induced release or Rab2A, Rab13, and Rab37 that stimulated release triggered by Ag). However, the majority of mutants inhibited the secretory process (Fig. 3). Among these groups, expression of only three mutants resulted in clear phenotypic traits. Unlike wt Rab37 and wt Rab38, their CA mutants translocated to the nucleus in resting or Ion/TPA-triggered cells (Fig. 4C). The reasons or physiological relevance of these nuclear translocations are presently unknown; however, nuclear sequestration of these mutants in Ion/TPA-treated cells may account for their selective inhibition of Ag-induced secretion.

Downloaded from http://jimmunol.org/ at Inst Superiore de Sanita-Roma on July 31, 2012

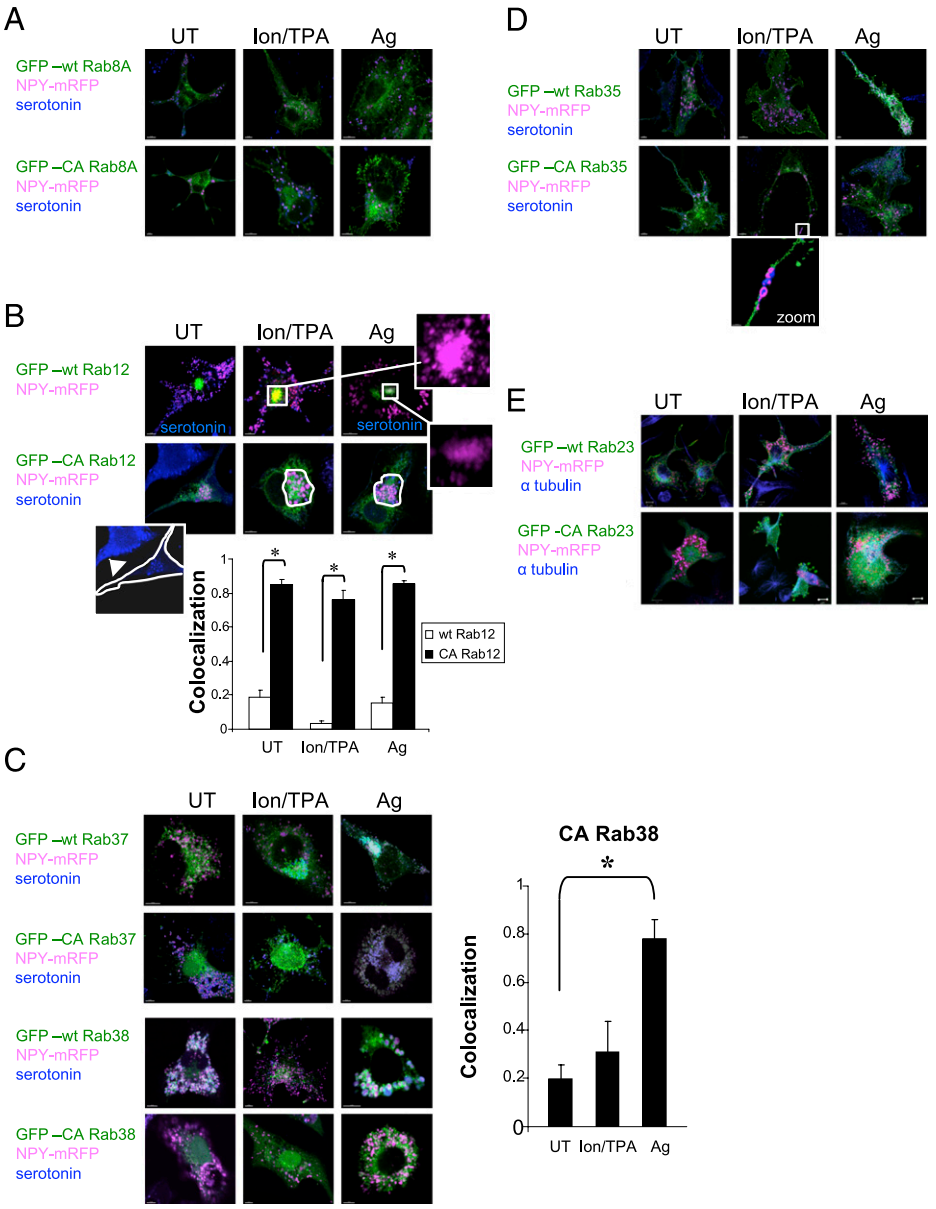

FIGURE 4. Phenotypic correlates of Rabs that impact exocytosis. Cells transiently cotransfected with NPY-mRFP and the indicated pEGFP wt or CA Rab mutants were left untreated (UT) or triggered with Ion/TPA or Ag for 10 min, as indicated (**A**–**E**). Cells were subsequently immunostained with anti-serotonin or anti-tubulin Abs, as indicated, followed by Hilyte Plus 647-conjugated secondary Abs. Deconvoluted fluorescence microscopy images are presented. Scale bars, 5 μm. *Insets* represent enlargements of the boxed areas. The *inset* and circled area in (B) depict perinuclear SGs. The arrow points to a nontransfected cell in which SGs are at the periphery, in contrast to the perinuclear SGs in the marked transfected cell. The extents of colocliza-tion between NPY-mRFP and Rab12 (B) or Rab38 (C) were quantified by the Zeiss LSM510 software. Data are means ± SEM from at least 45 cells. The *inset* in (D) corresponds to the boxed area reconstituted by Imaris software and depicts SGs captured in cell protrusions in Ion/TPA-triggered cells. *$p < 0.001$.

CA Rab35 selectively inhibited Ion/TPA-stimulated exocytosis (Fig. 3), and expression of this mutant induced membrane protrusions that became considerably longer upon Ion/TPA treatment (Fig. 4D). Furthermore, SGs appeared to be captured in these protrusions, lending further support to the notion of membrane protrusions serving as barriers of exocytosis (Fig. 4D). Images of cells expressing the remaining Rabs of these groups are presented in Supplemental Fig. 1B and 1C. Intriguingly, the majority of Rabs that affected selectively Ion/TPA-induced secretion are known to regulate steps along the biosynthetic/secretory pathway or bidirectional trafficking between the Golgi and endosomes. Included are Rab2A that regulates endoplasmic reticulum to Golgi trafficking (31) and Rab6A, Rab14, and Rab39A, which control the Golgi–endosome connection (40–42). These Rabs may therefore play a role in cargo delivery to the lysosomal SGs, hence their biogenesis.

Impact of wt Rabs on exocytosis

As discussed above, constitutively active Rab mutants may interfere with the functions displayed by their endogenous counterparts. As such, active mutants of Rabs that negatively regulate exocytosis may rather relieve inhibitory constraints. Expectedly in such a case is that wt forms will be more effective in inhibiting exocytosis than their CA mutant counterparts. To explore this possibility and search for potential negative regulators of exocytosis, we repeated our screen assessing the functional impacts of wt Rabs.

In most cases, expression of wt Rabs resulted in attenuated responses compared with their CA mutants (Fig. 3, Table III). However, some Rabs inhibited exocytosis exclusively in their wt forms, consistent with their assignment as negative regulators. The latter included Rab42 and Rab27A and, to a lesser extent, Rab11B, which inhibited exocytosis triggered by both Ion/TPA and Ag. Notably, quantitative analysis of the expression levels of Rab42 and Rab27A, wt and CA mutants, by flow cytometry, revealed that the average GFP fluorescence intensity of GFP-wt Rab42-expressing cells was 1.3-fold lower than the mean fluorescence of GFP-CA Rab42-expressing cells. In contrast, the mean fluorescence of GFP-wt Rab27A-expressing cells was 1.3 higher than that of their corresponding GFP-CA Rab27A-expressing cells (Supplemental Fig. 2). Therefore, this lack of correlation has ruled out the possibility of differences between

Downloaded from http://jimmunol.org/ at Inst Superiore de Sanita-Roma on July 31, 2012

Table III. Expression of wt Rabs affects NPY-mRFP release from triggered RBL cells

WT	Ion/TPA	±SEM	Ag	±SEM	*N*
GFP	100	0	100	0	
Rab1A	91	11.74	92	14.62	3
Rab2A	80	8.4	93	25.76	5
Rab3A	74	19.34	83	11.97	4
Rab4A	79	8.06	70	8.25	3
Rab5A	103	13.03	92	9.17	3
Rab6A	95	12.35	103	7.22	3
Rab7A	100	14.53	88	3.46	4
Rab8A	73	7.1	78	21.32	3
Rab8B	96	0.31	89	1.71	3
Rab9A	71	14.9	74	9.26	3
Rab10	51	2.08	81	12.59	3
Rab11A	58	15.81	65	26.28	3
Rab11B	72	2.23	78	7.19	3
Rab12	91	7.87	106	11.65	3
Rab13	98	12.38	165	62.48	3
Rab14	85	8.53	125	19.1	4
Rab15	81	1.5	93	1.58	3
Rab17	71	10.23	84	3.26	3
Rab18	95	4.38	108	17.41	3
Rab19	74	14.2	75	11.48	3
Rab20	76	10.03	89	10.13	4
Rab21	64	15.44	95	10.39	3
Rab22A	96	4.54	100	5.47	3
Rab23	77	16.04	87	4.24	3
Rab24	101	10.99	107	18.21	3
Rab25	104	10.86	89	4.42	3
Rab26	83	8.73	99	9.13	6
Rab27A	65	8.07	66	6.68	3
Rab27B	77	8.86	72	3.69	8
Rab28	67	5.9	113	2.95	3
Rab29	62	11.86	90	9.05	3
Rab30	96	6.39	95	3.26	3
Rab32	82	12.59	77	10.91	3
Rab33A	84	4.18	82	12.8	3
Rab34	101	5.4	110	13.44	3
Rab35	86	11.03	82	9.06	3
Rab36	93	4.45	109	21.18	3
Rab37	89	23.23	126	12.66	3
Rab38	80	14.07	52	8.77	3
Rab39A	77	4.82	75	2	3
Rab40	101	7.4	84	10.92	3
Rab41	90	1.02	107	38.01	3
Rab42	57	10.51	65	9.92	3
Rab43	68	15.42	117	14.56	3

RBL cells were transfected and treated as described under Table II, except that they were cotransfected with NPY-mRFP and either pEGFP or wt Rabs cDNAs. Data were analyzed as described under Table II.

these Rabs expression levels accounting for the remarkable divergence in their functional impacts.

Expression of CA Rab27A in RBL cells was previously shown to inhibit histamine release (33). We now show that also wt Rab27A inhibits secretion and to a higher extent. This observation thus adds to the growing body of evidence that highlight distinct roles and discrete mechanisms of action for Rab27A and Rab27B (43, 44). Moreover, these insights are fully consistent with findings in Rab27 KO mice that previously demonstrated a marked reduction in passive cutaneous allergic response in Rab27B KO mice, contrasted by an enhancement of this response in Rab27A KO mice dermis (34). It is noteworthy that we have also compared the relative expression levels of endogenous Rab27A and Rab27B by quantitative RT-PCR and found that consistent with their regulatory functions; both isoforms are expressed to similar levels in the RBL cells (data not shown). To substantiate this notion further and under our experimental setting, we attempted to downregulate the expression of Rab27A by RNAi and to assess the impact on exocytosis. However, only modest reduction in Rab27A expression was achieved, which was not associated with any effect on exocytosis (data not shown).

Our attempts to silence Rab42 were more successful. Microscopic analyses of cells cotransfected with NPY-mRFP and Rab42 silencer, and stained with Abs directed against Rab42, revealed that Rab42 was almost completely depleted in 40% of the NPY-mRFP–expressing cells (Fig. 5A). Monitoring NPY-mRFP release induced by either Ag or Ion/TPA revealed that it was increased by 17% (Fig. 5B). This effect was reproducible and significant. Moreover, taking into account the fraction of silenced cells, this potentiation does correspond to a 40% increase in secretion, consistent with the assignment of Rab42 as negative regulator of exocytosis.

Among the proteins that inhibited Ion/TPA-induced secretion in their wt conformations, the selective activity of Rab23 could be accounted for by the nuclear translocation of its CA mutant (Fig. 4E). However, the selective inhibition of Ion/TPA-triggered exocytosis manifested by Rab29, Rab21, Rab28, and Rab17 (Fig. 3, Table III) may implicate these Rabs as playing a regulatory role in cargo transport to the SG. Finally, Rab32, which is closely related to Rab38, exerted a modest inhibitory effect on secretion stimulated by Ag (Table III). Images depicting cells expressing negative regulating Rabs are presented in Supplemental Fig. 3.

Phylogenetic position of exocytosis regulating Rabs

We also analyzed whether the exocytosis regulating Rabs formed functional clusters on the Rab phylogenetic tree. Indeed, Rabs identified by our screen clustered into four branches (Fig. 6), one of which was already implicated in regulated secretory vesicle traffic (19). Furthermore, this analysis indicated that the mast cell exocytosis regulating Rabs comprised proteins shared by *Caenorhabditis elegans*, *Drosophila*, mice, and humans (i.e., Rab2A, Rab3A, Rab8A, Rab10, Rab14, Rab19, Rab21, Rab27A, Rab27B, Rab35, and Rab39A), as well as Rabs considered to be vertebrate or mammalian specific (i.e., Rab12, Rab13, Rab17, Rab20, Rab22A, Rab29, Rab38, Rab42, and Rab43). Hence, it is tempting to speculate that these groups represent increasing levels of regulatory complexity that evolved during evolution.

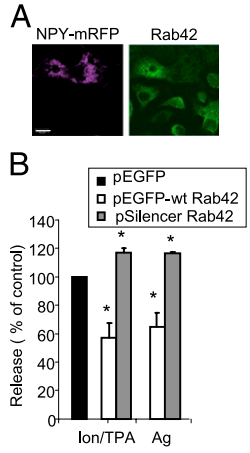

FIGURE 5. Triggered exocytosis is enhanced by Rab42 RNAi. Cells were transiently cotransfected with NPY-mRFP and pEGFP or pSilencer Rab42 cDNAs. Forty-eight hours later, cells were either immunostained with anti-Rab42 Abs, followed by Cy2-conjugated donkey anti-mouse IgG (**A**) or triggered with Ion/TPA or Ag for 30 min (**B**). Release is presented as percentage of release from control pEGFP-expressing cells. The data are means ± SEM of three independent experiments. *p = 0.046 (Ion/TPA); *p = 0.008 (Ag). Scale bar, 10 μm.

Downloaded from http://jimmunol.org/ at Inst Superiore de Sanita-Roma on July 31, 2012

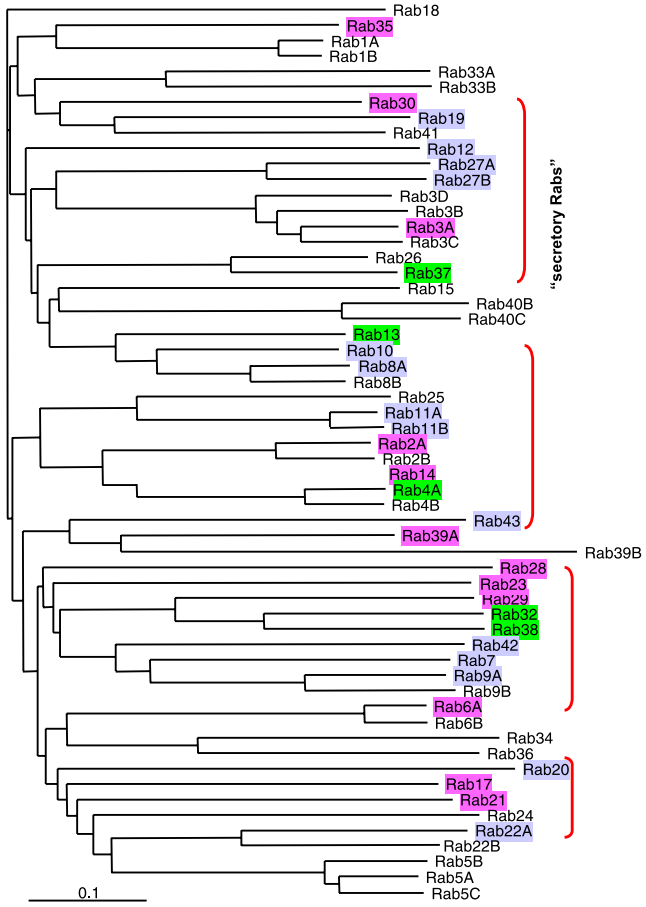

FIGURE 6. Phylogenetic distribution of exocytosis regulating Rabs. A molecular dendrogram of rat Rab family members was drawn by using the ClustalW program set at the default parameters (available at http://clustalw.ddbj.nig.ac.jp/top-e.html). Except for rat Rab43 (C-terminal 147 aa), full-length Rabs available in the public database were used for the phylogenetic analysis. Shaded in blue are Rabs that affected both Ag and Ion/TPA-triggered release (wt or CA mutants), shaded in purple are Rabs that affected only Ion/TPA-triggered release (wt or CA mutants), and shaded in green are Rabs that affected only Ag-triggered release (wt or CA mutants).

Table IV. Cytochalasin D affects NPY-mRFP release from triggered CA Rab mutants expressing RBL cells

CA Mutants	Ion/TPA	±SEM	Ag	±SEM	*N*
GFP	100	0	100	0	3
Rab1A	64	15.78	65	11.28	5
Rab2A	62	4.18	47	6.5	4
Rab3A	99	9.32	78	22.14	4
Rab4A	81	10.29	68	9.08	3
Rab5A	116	13.23	96	4.99	3
Rab6A	107	4.45	89	9.91	3
Rab7	69	4	58	6.49	3
Rab8A	59	5.73	52	13.51	3
Rab8B	81	1.04	96	5.36	3
Rab9A	54	8.35	58	5.48	3
Rab10	97	5.81	74	8.66	4
Rab11A	87	6.6	78	10.3	3
Rab11B	94	0	87	2	3
Rab12	54	0.77	67	3.28	6
Rab13	90	4.33	91	3.36	4
Rab14	55	2.58	56	5.69	4
Rab15	115	8.51	105	3.54	3
Rab17	112	3.99	102	16.08	3
Rab18	87	18.91	116	2.87	3
Rab19	72	7.86	65	4.41	4
Rab20	81	7.96	75	5.38	4
Rab21	111	2.67	107	20.7	3
Rab22A	74	6.6	74	3.75	3
Rab23	101	10.53	109	8.91	3
Rab24	88	5.42	104	3.59	3
Rab26	93	1.66	112	4.94	3
Rab27A	94	5.59	87	12.8	4
Rab27B	79	4.49	49	7.69	3
Rab28	83	5.64	95	15.55	3
Rab29	85	4.63	83	3.4	3
Rab30	113	6.33	81	13.58	3
Rab32	94	6.18	77	3.03	3
Rab33A	106	17.48	85	12.33	3
Rab34	116	15.66	120	16.26	3
Rab35	66	8.71	68	9.27	4
Rab36	96	3.5	95	10.32	3
Rab37	108	17.22	131	13.43	4
Rab38	110	15.5	102	7.15	3
Rab39A	100	6.19	72	7.6	3
Rab40	102	4.29	110	4.11	3
Rab41	70	14.46	89	4.23	3
Rab42	94	5.14	99	2.31	3
Rab43	86	7.37	65	8.09	3

RBL cells were transfected and treated as described under Table II, except that they were treated for 15 min with 10 μM cytochalasin D prior to cell trigger. Data were analyzed as described under Table II.

The role of actin in mediating Rab networks regulatory functions

Exocytosis involves the continuous reorganization of the actin cytoskeleton (13, 45), and the function of many Rabs is linked with actin rearrangements (19). Therefore, to explore the potential role of the actin skeleton in mediating Rab regulatory functions on exocytosis, we repeated our screen in the presence of cytochalasin D that disrupts the actin cytoskeleton by inhibiting actin polymerization. The relative release responses are presented in Table IV.

Cytochalasin D had no effect on the nonfunctional Rabs. However, the inhibitory (Rab10 and Rab11A) or stimulatory (Rab6A, Rab13, and Rab37) potencies of a number of Rabs were reduced or abolished, suggesting their functional dependence on an intact actin cytoskeleton (Fig. 7A). Strikingly, a second group of Rabs rather gained function under these conditions. This group included Rab2A, Rab14, Rab35, and Rab39A, which in the absence of cytochalasin D affected only Ion/TPA-induced secretion, whereas, in its presence, were able to restrain Ag-induced release (Fig. 7A).

We also directly visualized the actin rearrangements linked with exocytosis triggered by either stimulus by time-lapse microscopy of RBL cells transfected with Lifeact-EGFP. Resting cells displayed cortical actin and relatively thick and short protrusions that upon Ag addition were rapidly replaced by 2-fold longer and ~3-fold thinner protrusions (Fig. 7B, Supplemental Video 1). The latter dynamically ruffled to form macropinosomes that gradually removed the cortical actin (Fig. 7B, Supplemental Video 1). In contrast, although exposure to Ion/TPA resulted in cortical actin translocation to the cell interior, this process was neither associated with dynamic ruffling nor with macropinocytosis; instead, Ion/TPA-triggered cells displayed stiff protrusions (Supplemental Video 1). These data supported the premise of separate mechanisms mediating FcεRI or Ion/TPA-induced exocytosis that are associated with unique patterns of actin remodeling and are, respectively, regulated by distinct Rab networks.

Discussion

Design of unbiased gain-of-function screen based on coexpression of NPY-mRFP and GFP-active Rab mutants enabled us to identify 30 Rabs as modulators of regulated exocytosis in mast cells. Therefore, the number of Rabs now acknowledged as regulators of

Downloaded from http://jimmunol.org/ at Inst Superiore de Sanita-Roma on July 31, 2012

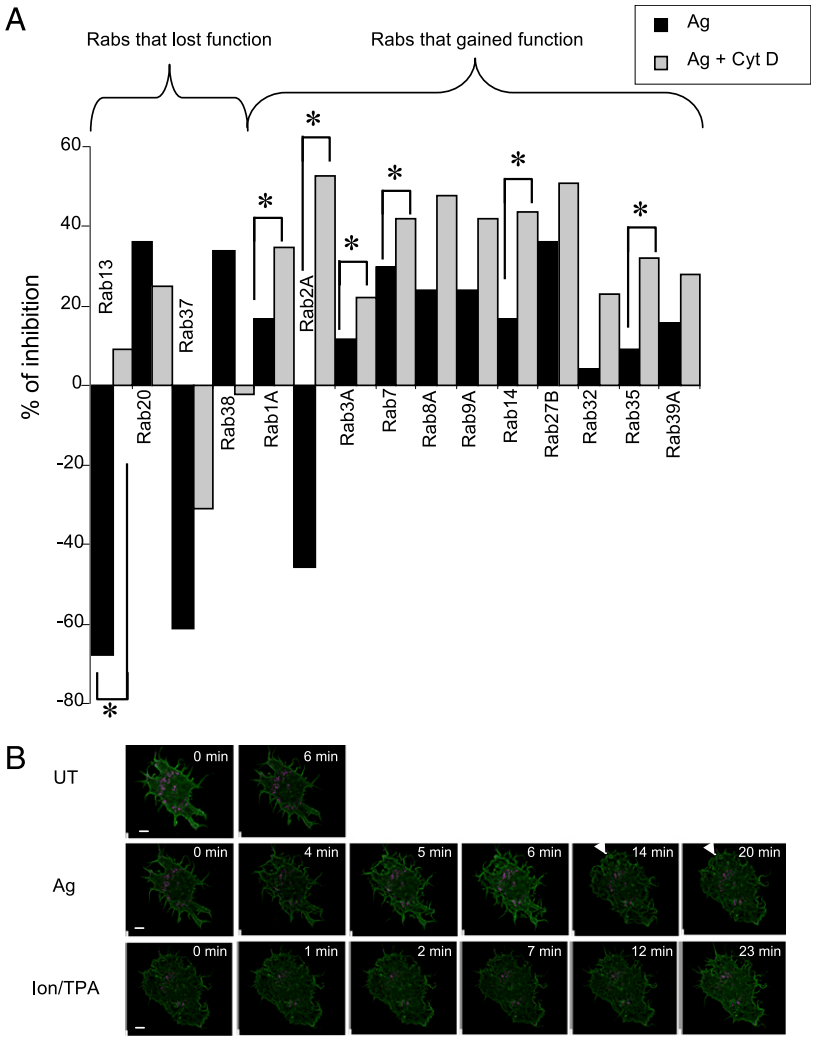

FIGURE 7. The role of actin in mediating Rab functional impacts. RBL cells were cotransfected with NPY-mRFP and either pEGFP or the indicated pEGFP-CA Rab mutant cDNAs. Cells were treated as described under Fig. 3, except that they were preincubated for 15 min with 10 μM cytochalasin D before trigger. Release of NPY-mRFP was measured and compared with the release from control pEGFP-expressing cells (summarized in Table IV). The extents of inhibition of Ag-triggered NPY-mRFP release by the CA Rab mutants, in the absence or presence of cytochalasin D (Cyt D) (Table II versus Table IV) are depicted (**A**). $^*p < 0.1$; inhibition < 0 corresponds to enhancement of secretion. In (**B**), cells were cotransfected with pEGFP-Lifeact and NPY-mRFP and imaged before (UT) and after trigger with Ag, followed by three washes, and stimulation with Ion/TPA, as described under *Materials and Methods*. Time-lapse fluorescence microscopy images were captured and deconvoluted. The arrowheads point to macropinosomes forming upon Ag trigger. Scale bar, 5 μM. The video is presented in the supplemental material.

this process by far exceeds previous notions. Out of this list, four Rabs (Rab37, Rab3A, Rab27A, and Rab27B (33–35, 46, 47)) were already reported in this respect, and their recognition by our screen lends credibility to the novel Rabs identified. Our results also demonstrate that Rab function is isoform specific. Hence, in a few cases, only a single isoform affected exocytosis (i.e., Rab8A), whereas in other cases, cognate isoforms seem to display opposite functions (i.e., Rab27 and Rab11).

Intriguingly, our screen could also resolve Rabs that exclusively affected FcεRI-mediated secretion or secretion stimulated by the combination of Ion/TPA. In this regard, Rabs that selectively modulated Ag-induced release may be involved in controlling FcεRI trafficking or its downstream signaling effectors. However, identification of Rabs as selective modulators of Ion/TPA-stimulated exocytosis was rather unexpected, because the latter is traditionally thought to constitute a downstream step of the FcεRI-stimulated release. In contrast, our results are compatible with a model whereby two distinct mechanisms mediate Ag or Ion/TPA-induced secretion and accordingly engage different Rabs (see model; Fig. 8). This two-arm model is supported by the fact that the actin rearrangements we characterized for Ag or Ion/TPA-induced secretion were previously attributed to kiss-and-run and full exocytosis, respectively (13). Therefore, our results are compatible with a model whereby Ion/TPA promotes full exocytosis, whereas Ag triggers secretion by a kiss-and-run mechanism. Indeed, careful analysis of the dynamics of the secretory process led to the conclusion that the frequency of kiss-and-run exocytosis is 2-fold higher than that of full exocytosis in Ag-triggered RBL cells (48). Moreover, in the presence of cytochalasin D, which was previously shown to shift kiss-and-run to full exocytosis (49), the Ion/TPA-inhibitory Rabs turned inhibitory toward Ag.

Interestingly, the Ion/TPA-modulating Rab network comprises Rabs primarily involved in controlling transport along the biosynthetic/secretory pathway and its interface with the endocytic system. This finding may suggest that during compound exocytosis, stimulated by Ion/TPA, newly formed immature SGs (ISGs), largely affected by biosynthetic Rabs, do also release their contents by homotypic fusion with pre-existing mature SGs (Fig. 8).

The network of Rab GTPases identified as modulators of both Ag and Ion/TPA-induced exocytosis segregates into three groups. The first group comprises Rabs that localized to the SGs (i.e., Rab7, Rab9A, Rab19, Rab27A, Rab27B, Rab42, and Rab43) and are therefore likely to regulate final steps of exocytosis, such as priming, docking, and fusion with the plasma membrane, which are shared by kiss-and-run and full exocytosis mechanisms. The relatively large number of Rabs implicated is consistent with proteomic analyses of several types of secretory cells that revealed the presence of unexpectedly large numbers of Rabs on secretory vesicles (19). Moreover, these findings imply the involvement of diverse yet functionally redundant Rab effectors, which may account for the restricted inhibition that is imposed by the expression of single CA mutants. Consistent with this notion is the

Downloaded from http://jimmunol.org/ at Inst Superiore de Sanita-Roma on July 31, 2012

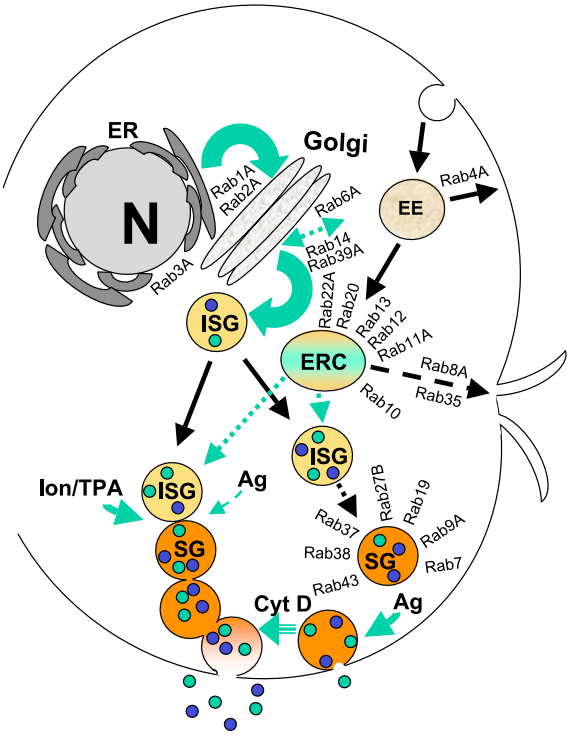

FIGURE 8. A model for the selective trigger-dependent regulation of mast cell secretion by Rab GTPases. According to our model, Ag and Ion/TPA provoke secretion by distinct mechanisms. Ag stimulates primarily kiss-and-run exocytosis, where only plasma membrane docked SGs release part of their contents through a transient fusion pore. Ion/TPA induces compound exocytosis, involving homotypic fusion of SGs and their full exocytosis. Moreover, newly formed ISGs also release their contents by fusing with mature SGs. In the presence of cytochalasin D (Cyt D), Ag-induced kiss-and-run exocytosis is replaced by compound exocytosis. According to this model, Rabs that reside on or are recruited to the SGs, as well as Rabs that regulate transport from the ERC, regulate final steps of exocytosis, which are shared by both exocytic mechanisms. Rabs that connect the biosynthetic and endocytic systems mediate the biogenesis of ISGs and accordingly affect only Ion/TPA-induced secretion or secretion by either stimulus in the presence of Cyt D. Shown in this model are Rabs identified as positive regulators of exocytosis.

observation that complete absence of all four Rab3 isoforms results in only a 30% reduction in Ca^{2+}-triggered neurotransmitter release (50). Within this first group of general modulators, Rab27A and Rab42 were assigned the role of negative regulators of exocytosis. Indeed, Rab27A was already implicated in playing such role in mast cells (34). However, the function of Rab42 in mast cells has not been studied before, and its identification as a negative regulator of mast cells exocytosis is intriguing.

Confusingly, rodent Rab42 (accession number AB232641.1; http://www.ncbi.nlm.nih.gov/nuccore/AB232641.1) is in fact the synonym of Rab7B (accession number, NP_663484; http://www.ncbi.nlm.nih.gov/protein/NP_663484) that is distinct from the human Rab42, the homolog of rodent Rab43. Rab7B has been implicated in controlling cycling cargo transport between the TGN and late endosomes/lysosomes (51). Furthermore, RNAi of Rab7B in HeLa cells resulted in the enhanced secretion of β-hexosaminidase (51). Finally, in macrophages, this Rab homolog suppresses TLR4 and TLR9 proinflammatory signaling (52, 53). Therefore, our recognition of Rab42/Rab7B as negative regulator of mast cell secretion is consistent with this Rab anti-inflammatory function in macrophages and suggests a broader role for this Rab in negative regulation of inflammatory responses.

The second group consists of Rab12, whose CA mutant enforced SG clustering at a perinuclear region, suggesting involvement of this Rab in SGs transport. Consistent with this finding, Rab12 was implicated in accelerating vesicular transport from the cell periphery to the perinuclear centrosome region (54) and was recently shown by us to control transport from the ERC to lysosomes (38). Finally, and in line with the perinuclear positioning of the SGs, the third group of exocytosis-modulating Rabs includes regulators of transport through the ERC (i.e., Rab8A, Rab10, Rab11A, Rab20, and Rab22A). Inhibition of exocytosis by active Rab mutants that enhance recycling through the ERC (i.e., the latter group) can be accounted for by at least two nonexclusive mechanisms. First, a genetically manipulated mouse model suggests that stimulated recycling may inhibit exocytosis by competing with the SGs for the plasma membrane fusion machinery (17). Such competition for membrane SNAREs may serve a physiological role in coordinating mast cell migration, which depends on polarized endocytic recycling (55), with exocytosis. In accordance, Liu et al. (56) demonstrated that migrating RBL cells do not secrete and when they secrete they stiffen. Along this line of thought, RBL cells display both polarized and receptor-stimulated endocytic recycling (57, 58), and we show in this paper that they also express Rab13, Rab17, Rab20, and Rab25, which are all implicated in polarized transport in epithelial cells. Alternatively, the ERC may mediate acquisition of exocytosis competence by the SGs in analogy to its role in exocytosis of CTL granules (59). In such a scenario, enhancing the flow toward the plasma membrane is postulated to perturb the interaction between the ERC and the SGs, thereby interfering with their exocytosis competence acquisition process. The latter possibility is supported by the detection of SGs at the perinuclear region in activated cells, where they colocalize with Rab11A (Supplemental Fig. 1A) (35) and their perinuclear accumulation and immobilization in Rab12- and CA Rab12-expressing cells.

In conclusion, our screen identified a Rab network consisting of 30 Rabs, 26 of which were hitherto unappreciated as regulators of mast cell exocytosis. Unveiling this network provides invaluable tools for decoding the distinct mechanisms and pathways that are involved in the biogenesis and degranulation of mast cell SGs.

Acknowledgments

We thank Dr. U. Ashery for the generous gift of cDNA. We thank Drs. L. Mittleman, M. Shaharbani, and Y. Zilberstein for invaluable assistance with microscopy and image analyses and Dr. M. Pasmanik-Chor for assistance with bioinformatics analysis. We also thank Dr. Joseph Orly for critical reading of this manuscript.

Disclosures

The authors declare no competing financial interests.

References

1. Weller, K., K. Foitzik, R. Paus, W. Syska, and M. Maurer. 2006. Mast cells are required for normal healing of skin wounds in mice. *FASEB J.* 20: 2366–2368.
2. Tsai, M., M. Grimbaldeston, and S. J. Galli. 2011. Mast cells and immunoregulation/immunomodulation. *Adv. Exp. Med. Biol.* 716: 186–211.
3. Schwartz, L. B., and K. F. Austen. 1980. Enzymes of the mast cell granule. *J. Invest. Dermatol.* 74: 349–353.
4. Suárez-Quian, C. A. 1987. The distribution of four lysosomal integral membrane proteins (LIMPs) in rat basophilic leukemia cells. *Tissue Cell* 19: 495–504.
5. Griffiths, G. M. 1996. Secretory lysosomes—a special mechanism of regulated secretion in haemopoietic cells. *Trends Cell Biol.* 6: 329–332.
6. Kalesnikoff, J., and S. J. Galli. 2008. New developments in mast cell biology. *Nat. Immunol.* 9: 1215–1223.
7. Ott, V. L., and J. C. Cambier. 2000. Activating and inhibitory signaling in mast cells: new opportunities for therapeutic intervention? *J. Allergy Clin. Immunol.* 106: 429–440.

Downloaded from http://jimmunol.org/ at Inst Superiore de Sanita-Roma on July 31, 2012

8. Rivera, J., N. A. Fierro, A. Olivera, and R. Suzuki. 2008. New insights on mast cell activation via the high affinity receptor for IgE. *Adv. Immunol.* 98: 85–120.
9. Benhamou, M., and U. Blank. 2010. Stimulus-secretion coupling by high-affinity IgE receptor: new developments. *FEBS Lett.* 584: 4941–4948.
10. Kashiwakura, J., I. M. Otani, and T. Kawakami. 2011. Monomeric IgE and mast cell development, survival and function. *Adv. Exp. Med. Biol.* 716: 29–46.
11. Puri, N., and P. A. Roche. 2008. Mast cells possess distinct secretory granule subsets whose exocytosis is regulated by different SNARE isoforms. *Proc. Natl. Acad. Sci. USA* 105: 2580–2585.
12. Raposo, G., D. Tenza, S. Mecheri, R. Peronet, C. Bonnerot, and C. Desaymard. 1997. Accumulation of major histocompatibility complex class II molecules in mast cell secretory granules and their release upon degranulation. *Mol. Biol. Cell* 8: 2631–2645.
13. Deng, Z., T. Zink, H. Y. Chen, D. Walters, F. T. Liu, and G. Y. Liu. 2009. Impact of actin rearrangement and degranulation on the membrane structure of primary mast cells: a combined atomic force and laser scanning confocal microscopy investigation. *Biophys. J.* 96: 1629–1639.
14. Pickett, J. A., and J. M. Edwardson. 2006. Compound exocytosis: mechanisms and functional significance. *Traffic* 7: 109–116.
15. Blank, U. 2011. The mechanisms of exocytosis in mast cells. *Adv. Exp. Med. Biol.* 716: 107–122.
16. Baram, D., R. Adachi, O. Medalia, M. Tuvim, B. F. Dickey, Y. A. Mekori, and R. Sagi-Eisenberg. 1999. Synaptotagmin II negatively regulates Ca^{2+}-triggered exocytosis of lysosomes in mast cells. *J. Exp. Med.* 189: 1649–1658.
17. Tiwari, N., C.-C. Wang, C. Brochetta, G. Ke, F. Vita, Z. Qi, J. Rivera, M. R. Soranzo, G. Zabucchi, W. Hong, and U. Blank. 2008. VAMP-8 segregates mast cell-preformed mediator exocytosis from cytokine trafficking pathways. *Blood* 111: 3665–3674.
18. Woska, J. R., Jr., and M. E. Gillespie. 2012. SNARE complex-mediated degranulation in mast cells. *J. Cell. Mol. Med.* 16: 649–656.
19. Fukuda, M. 2008. Regulation of secretory vesicle traffic by Rab small GTPases. *Cell. Mol. Life Sci.* 65: 2801–2813.
20. Tsuboi, T., and M. Fukuda. 2006. Rab3A and Rab27A cooperatively regulate the docking step of dense-core vesicle exocytosis in PC12 cells. *J. Cell Sci.* 119: 2196–2203.
21. Kanno, E., K. Ishibashi, H. Kobayashi, T. Matsui, N. Ohbayashi, and M. Fukuda. 2010. Comprehensive screening for novel rab-binding proteins by GST pull-down assay using 60 different mammalian Rabs. *Traffic* 11: 491–507.
22. Itoh, T., M. Satoh, E. Kanno, and M. Fukuda. 2006. Screening for target Rabs of TBC (Tre-2/Bub2/Cdc16) domain-containing proteins based on their Rab-binding activity. *Genes Cells* 11: 1023–1037.
23. Kuroda, T. S., and M. Fukuda. 2004. Rab27A-binding protein Slp2-a is required for peripheral melanosome distribution and elongated cell shape in melanocytes. *Nat. Cell Biol.* 6: 1195–1203.
24. Nokes, R. L., I. C. Fields, R. N. Collins, and H. Fölsch. 2008. Rab13 regulates membrane trafficking between TGN and recycling endosomes in polarized epithelial cells. *J. Cell Biol.* 182: 845–853.
25. Zacchi, P., H. Stenmark, R. G. Parton, D. Orioli, F. Lim, A. Giner, I. Mellman, M. Zerial, and C. Murphy. 1998. Rab17 regulates membrane trafficking through apical recycling endosomes in polarized epithelial cells. *J. Cell Biol.* 140: 1039–1053.
26. Das Sarma, J., B. E. Kaplan, D. Willemsen, and M. Koval. 2008. Identification of rab20 as a potential regulator of connexin 43 trafficking. *Cell Commun. Adhes.* 15: 65–74.
27. Goldenring, J. R., K. R. Shen, H. D. Vaughan, and I. M. Modlin. 1993. Identification of a small GTP-binding protein, Rab25, expressed in the gastrointestinal mucosa, kidney, and lung. *J. Biol. Chem.* 268: 18419–18422.
28. Stenmark, H., R. G. Parton, O. Steele-Mortimer, A. Lütcke, J. Gruenberg, and M. Zerial. 1994. Inhibition of rab5 GTPase activity stimulates membrane fusion in endocytosis. *EMBO J.* 13: 1287–1296.
29. Ren, M., G. Xu, J. Zeng, C. De Lemos-Chiarandini, M. Adesnik, and D. D. Sabatini. 1998. Hydrolysis of GTP on rab11 is required for the direct delivery of transferrin from the pericentriolar recycling compartment to the cell surface but not from sorting endosomes. *Proc. Natl. Acad. Sci. USA* 95: 6187–6192.
30. Neeft, M., M. Wieffer, A. S. de Jong, G. Negroiu, C. H. Metz, A. van Loon, J. Griffith, J. Krijgsveld, N. Wulffraat, H. Koch, et al. 2005. Munc13-4 is an effector of rab27a and controls secretion of lysosomes in hematopoietic cells. *Mol. Biol. Cell* 16: 731–741.
31. Tisdale, E. J. 1999. A Rab2 mutant with impaired GTPase activity stimulates vesicle formation from pre-Golgi intermediates. *Mol. Biol. Cell* 10: 1837–1849.
32. Jacobs, D. T., R. Weigert, K. D. Grode, J. G. Donaldson, and R. E. Cheney. 2009. Myosin Vc is a molecular motor that functions in secretory granule trafficking. *Mol. Biol. Cell* 20: 4471–4488.
33. Goishi, K., K. Mizuno, H. Nakanishi, and T. Sasaki. 2004. Involvement of Rab27 in antigen-induced histamine release from rat basophilic leukemia 2H3 cells. *Biochem. Biophys. Res. Commun.* 324: 294–301.
34. Mizuno, K., T. Tolmachova, D. S. Ushakov, M. Romao, M. Abrink, M. A. Ferenczi, G. Raposo, and M. C. Seabra. 2007. Rab27b regulates mast cell granule dynamics and secretion. *Traffic* 8: 883–892.
35. Elstak, E. D., M. Neeft, N. T. Nehme, J. Voortman, M. Cheung, M. Goodarzifard, H. C. Gerritsen, P. M. van Bergen En Henegouwen, I. Callebaut, G. de Saint Basile, and P. van der Sluijs. 2011. The munc13-4-rab27 complex is specifically required for tethering secretory lysosomes at the plasma membrane. *Blood* 118: 1570–1578.
36. Hattula, K., J. Furuhjelm, J. Tikkanen, K. Tanhuanpää, P. Laakkonen, and J. Peränen. 2006. Characterization of the Rab8-specific membrane traffic route linked to protrusion formation. *J. Cell Sci.* 119: 4866–4877.
37. Schuck, S., M. J. Gerl, A. Ang, A. Manninen, P. Keller, I. Mellman, and K. Simons. 2007. Rab10 is involved in basolateral transport in polarized Madin–Darby canine kidney cells. *Traffic* 8: 47–60.
38. Matsui, T., T. Itoh, and M. Fukuda. 2011. Small GTPase Rab12 regulates constitutive degradation of transferrin receptor. *Traffic* 12: 1432–1443.
39. Weigert, R., A. C. Yeung, J. Li, and J. G. Donaldson. 2004. Rab22a regulates the recycling of membrane proteins internalized independently of clathrin. *Mol. Biol. Cell* 15: 3758–3770.
40. Mallard, F., B. L. Tang, T. Galli, D. Tenza, A. Saint-Pol, X. Yue, C. Antony, W. Hong, B. Goud, and L. Johannes. 2002. Early/recycling endosomes-to-TGN transport involves two SNARE complexes and a Rab6 isoform. *J. Cell Biol.* 156: 653–664.
41. Junutula, J. R., A. M. De Maziére, A. A. Peden, K. E. Ervin, R. J. Advani, S. M. van Dijk, J. Klumperman, and R. H. Scheller. 2004. Rab14 is involved in membrane trafficking between the Golgi complex and endosomes. *Mol. Biol. Cell* 15: 2218–2229.
42. Chen, T., Y. Han, M. Yang, W. Zhang, N. Li, T. Wan, J. Guo, and X. Cao. 2003. Rab39, a novel Golgi-associated Rab GTPase from human dendritic cells involved in cellular endocytosis. *Biochem. Biophys. Res. Commun.* 303: 1114–1120.
43. Ostrowski, M., N. B. Carmo, S. Krumeich, I. Fanget, G. Raposo, A. Savina, C. F. Moita, K. Schauer, A. N. Hume, R. P. Freitas, et al. 2010. Rab27a and Rab27b control different steps of the exosome secretion pathway. *Nat. Cell Biol.* 12: 19–30, 1–13.
44. Johnson, J. L., A. A. Brzezinska, T. Tolmachova, D. B. Munafo, B. A. Ellis, M. C. Seabra, H. Hong, and S. D. Catz. 2010. Rab27a and Rab27b regulate neutrophil azurophilic granule exocytosis and NADPH oxidase activity by independent mechanisms. *Traffic* 11: 533–547.
45. Föger, N., A. Jenckel, Z. Orinska, K.-H. Lee, A. C. Chan, and S. Bulfone-Paus. 2011. Differential regulation of mast cell degranulation versus cytokine secretion by the actin regulatory proteins Coronin1a and Coronin1b. *J. Exp. Med.* 208: 1777–1787.
46. Masuda, E. S., Y. Luo, C. Young, M. Shen, A. B. Rossi, B. C. Huang, S. Yu, M. K. Bennett, D. G. Payan, and R. H. Scheller. 2000. Rab37 is a novel mast cell specific GTPase localized to secretory granules. *FEBS Lett.* 470: 61–64.
47. Smith, J., N. Thompson, J. Thompson, J. Armstrong, B. Hayes, A. Crofts, J. Squire, C. Teahan, L. Upton, and R. Solari. 1997. Rat basophilic leukaemia (RBL) cells overexpressing Rab3a have a reversible block in antigen-stimulated exocytosis. *Biochem. J.* 323: 321–328.
48. Williams, R. M., and W. W. Webb. 2000. Single granule pH cycling in antigen-induced mast cell secretion. *J. Cell Sci.* 113: 3839–3850.
49. Doreian, B. W., T. G. Fulop, and C. B. Smith. 2008. Myosin II activation and actin reorganization regulate the mode of quantal exocytosis in mouse adrenal chromaffin cells. *J. Neurosci.* 28: 4470–4478.
50. Schlüter, O. M., F. Schmitz, R. Jahn, C. Rosenmund, and T. C. Südhof. 2004. A complete genetic analysis of neuronal Rab3 function. *J. Neurosci.* 24: 6629–6637.
51. Progida, C., L. Cogli, F. Piro, A. De Luca, O. Bakke, and C. Bucci. 2010. Rab7b controls trafficking from endosomes to the TGN. *J. Cell Sci.* 123: 1480–1491.
52. Wang, Y., T. Chen, C. Han, D. He, H. Liu, H. An, Z. Cai, and X. Cao. 2007. Lysosome-associated small Rab GTPase Rab7b negatively regulates TLR4 signaling in macrophages by promoting lysosomal degradation of TLR4. *Blood* 110: 962–971.
53. Yao, M., X. Liu, D. Li, T. Chen, Z. Cai, and X. Cao. 2009. Late endosome/lysosome-localized Rab7b suppresses TLR9-initiated proinflammatory cytokine and type I IFN production in macrophages. *J. Immunol.* 183: 1751–1758.
54. Iida, H., M. Noda, T. Kaneko, M. Doiguchi, and T. Mōri. 2005. Identification of rab12 as a vesicle-associated small GTPase highly expressed in Sertoli cells of rat testis. *Mol. Reprod. Dev.* 71: 178–185.
55. Veale, K. J., C. Offenhäuser, S. P. Whittaker, R. P. Estrella, and R. Z. Murray. 2010. Recycling endosome membrane incorporation into the leading edge regulates lamellipodia formation and macrophage migration. *Traffic* 11: 1370–1379.
56. Liu, Z. Y., J. I. Young, and E. L. Elson. 1987. Rat basophilic leukemia cells stiffen when they secrete. *J. Cell Biol.* 105: 2933–2943.
57. Wu, M., T. Baumgart, S. Hammond, D. Holowka, and B. Baird. 2007. Differential targeting of secretory lysosomes and recycling endosomes in mast cells revealed by patterned antigen arrays. *J. Cell Sci.* 120: 3147–3154.
58. Naal, R. M., E. P. Holowka, B. Baird, and D. Holowka. 2003. Antigen-stimulated trafficking from the recycling compartment to the plasma membrane in RBL mast cells. *Traffic* 4: 190–200.
59. Ménager, M. M., G. Ménasché, M. Romao, P. Knapnougel, C. H. Ho, M. Garfa, G. Raposo, J. Feldmann, A. Fischer, and G. de Saint Basile. 2007. Secretory cytotoxic granule maturation and exocytosis require the effector protein hMunc13-4. *Nat. Immunol.* 8: 257–267.

Downloaded from http://jimmunol.org/ at Inst Superiore de Sanita-Roma on July 31, 2012

Legends to supplementary information

Supplemental Figure 1: Subcellular localization of Rabs whose CA mutants affect exocytosis.

Confocal fluorescence microscopy images of RBL cells co-transfected with NPY-mRFP and the indicated pEGFP-wt or CA Rab GTPases and either left untreated (UT), or stimulated for 10 minutes with 50 ng/ml of DNP-HSA (Ag) or 5 μM Ca^{2+} ionophore and 50 nM TPA (Ion/TPA) as indicated. Cells were immunostained with monoclonal anti serotonin or anti α tubulin or anti TGN38 (BD Biosciences, Franklin Lakes, NJ), antibodies followed by Hilyte Plus 647-conjugated secondary antibodies or in the case of Flag-wt Rab27B, with monoclonal anti Flag (Sigma Aldrich, St-Louis) and polyclonal anti serotonin (Oncogene, Cambridge, MA) followed by Hilyte Plus 647-conjugated goat anti rabbit IgG (Anaspec, Fremont, CA) and Cy2-conjugated donkey anti mouse IgG (Jackson ImmunoResearch, West Grove, PA) antibodies, or stained with Hoechst (nucleus), as indicated. The insets correspond to the boxed areas. Enlargements of Rab7, Rab9A and Rab19 were reconstituted by the Imaris software. In the case of Rab11A, insets demonstrate accumulation of SGs at the perinuclear region in activated cells. In the case of Rab27B, the arrows point to its plasma membrane location in triggered cells. In (**A**) are deconvoluted images of cells expressing Rabs that affected both Ag and Ion/TPA-triggered secretion, Bars = 5 μm; in (**B**) are images of cells expressing Rabs that affected only Ag-induced secretion, Bars = 10 μm and in (**C**) are images of cells expressing Rabs that affected exclusively Ion/TPA-induced secretion, Bars = 10 μm.

Supplemental Figure 2: Analysis of the expression levels of Rab42 and Rab27A wt and CA mutants.

RBL cells were transiently transfected with pEGFP-wt Rab27A, or pEGFP-wt Rab42 or their pEGFP-CA mutants cDNAs. Twenty-four hours later, cells were washed three times in ice-cold PBS. Cells fluorescence was analyzed by a FACSort flow cytometer and the average pEGFP fluorescence intensities were calculated.

Supplemental Figure 3: Subcellular localization of Rabs whose wt forms affect exocytosis.

Deconvolution of confocal fluorescence microscopy images of RBL cells co-transfected with NPY-mRFP and the indicated pEGFP-wt or CA Rab GTPases and either left untreated (UT), or triggered with Ag or Ion/TPA, as indicated. Cells were processed as described under Figure S1. Bars = 5 μm.

Supplemental Table I: Fifty-seven Rab GTPases are expressed endogenously in RBL cells.

The endogenous expression profile of Rab GTPases was determined by RT-PCR, using the primers listed under Materials and Methods.

Supplemental Video 1: Actin rearrangement conferred upon cell triggering by antigen or Ion/TPA.

RBL cells were co-transfected with pEGFP-Lifeact (25 μg) and NPY-mRFP (25 μg) and seeded at $2x10^5$ cells/chamber for twenty-four hours in the presence of DNP specific IgE (1 μg/ml). Twenty-four hours later cells were washed with Tyrode buffer (time 0) as described under Methods, and images were captured by Zeiss510 every 60 seconds for 6 minutes. Cells were then washed and triggered by Ag and images captured every 15 seconds (from 15.27 to 58 minutes). Cells were then washed 3 times and triggered with Ion/TPA (from 62 minutes to the end of the Video).

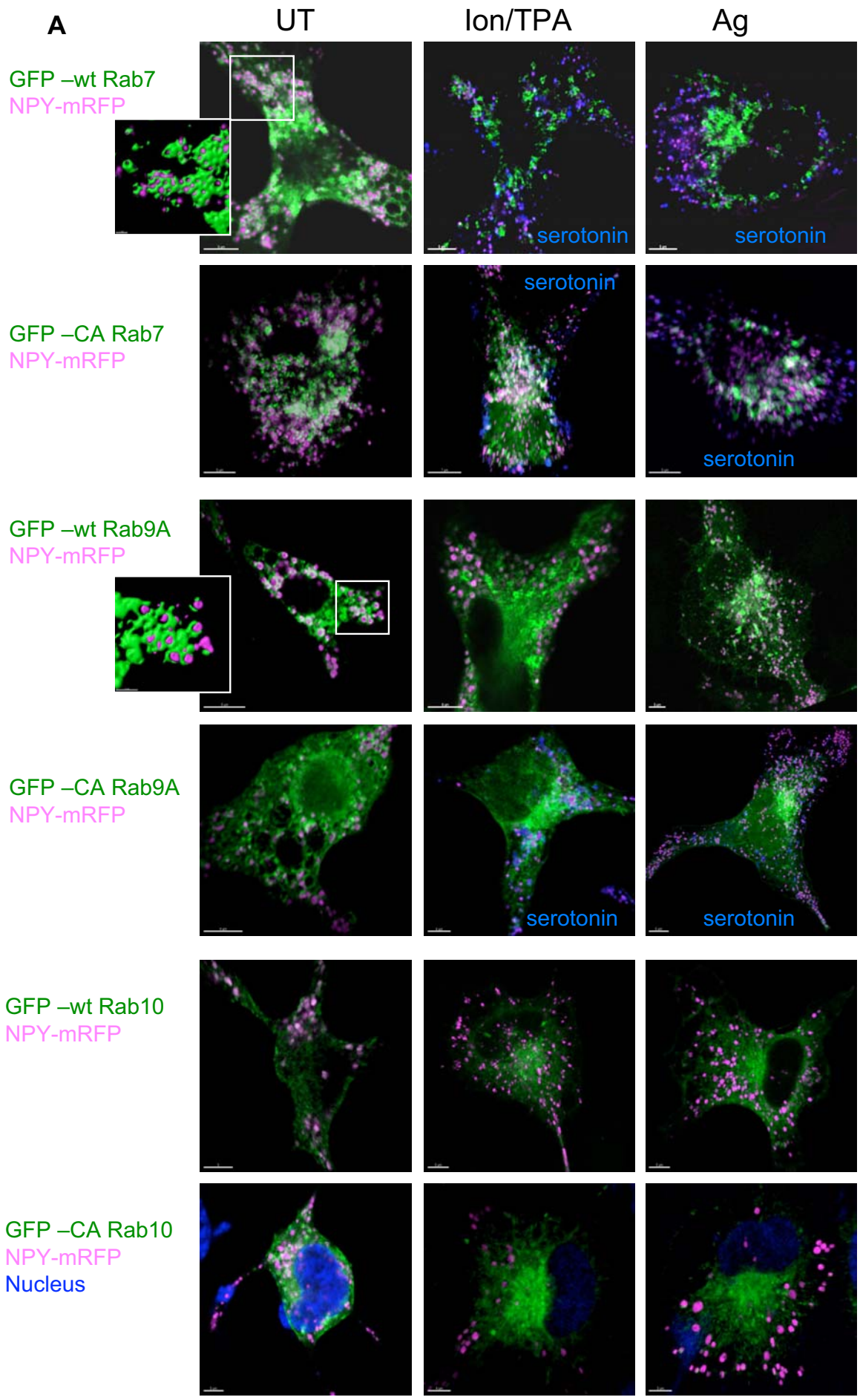

Supplemental Fig. S1A

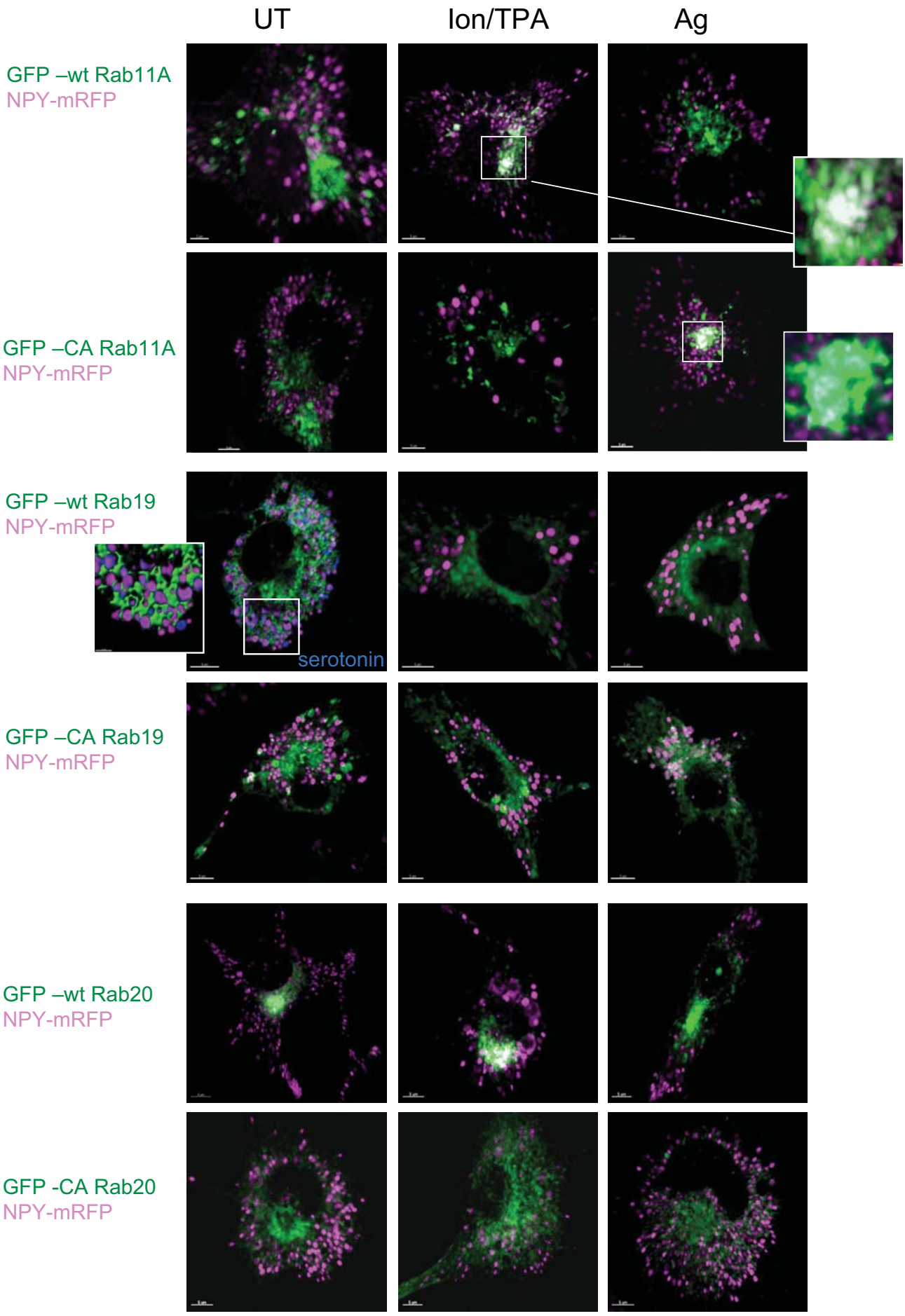

Supplemental Fig. S1A continued

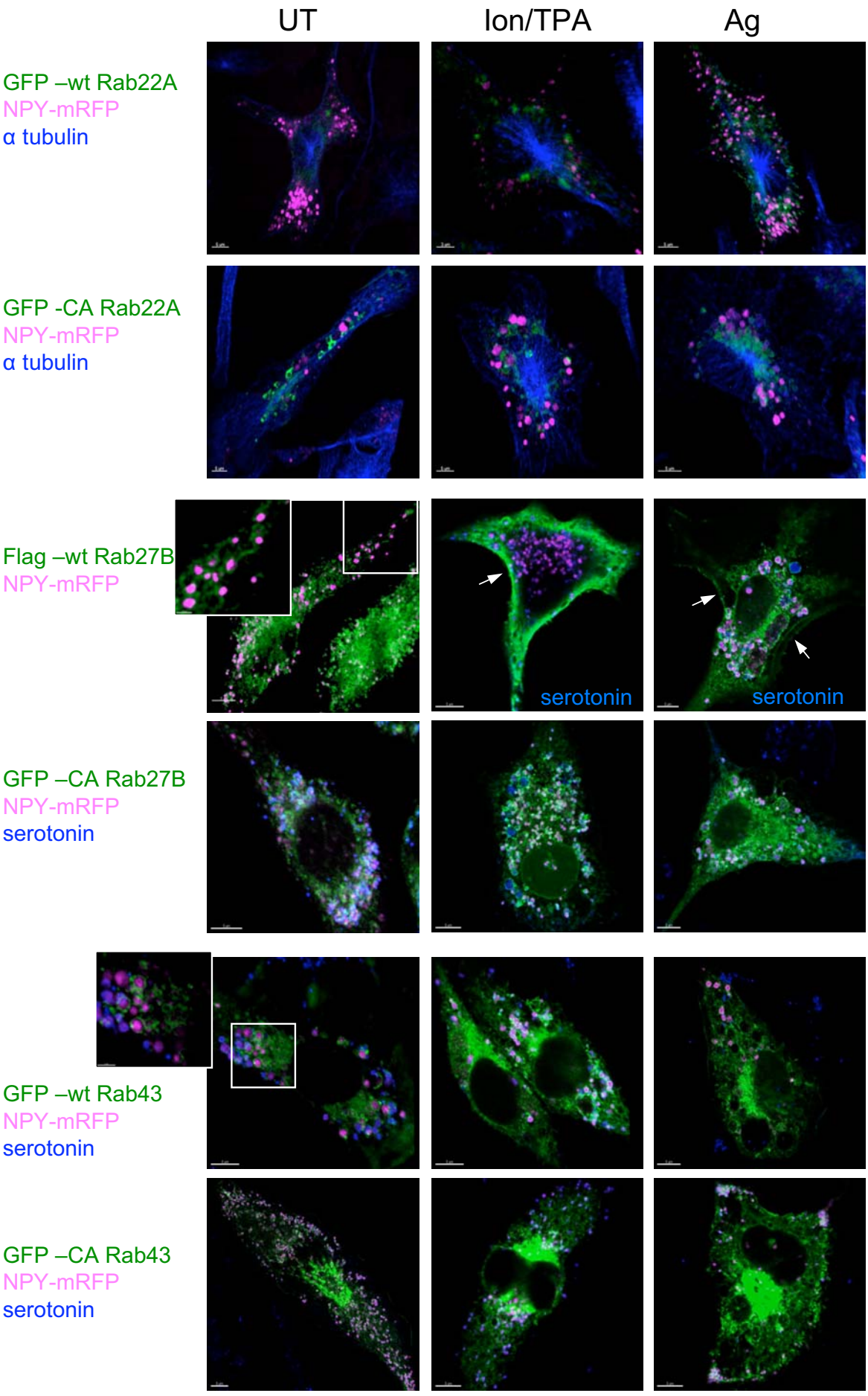

Supplemental Fig. S1A continued

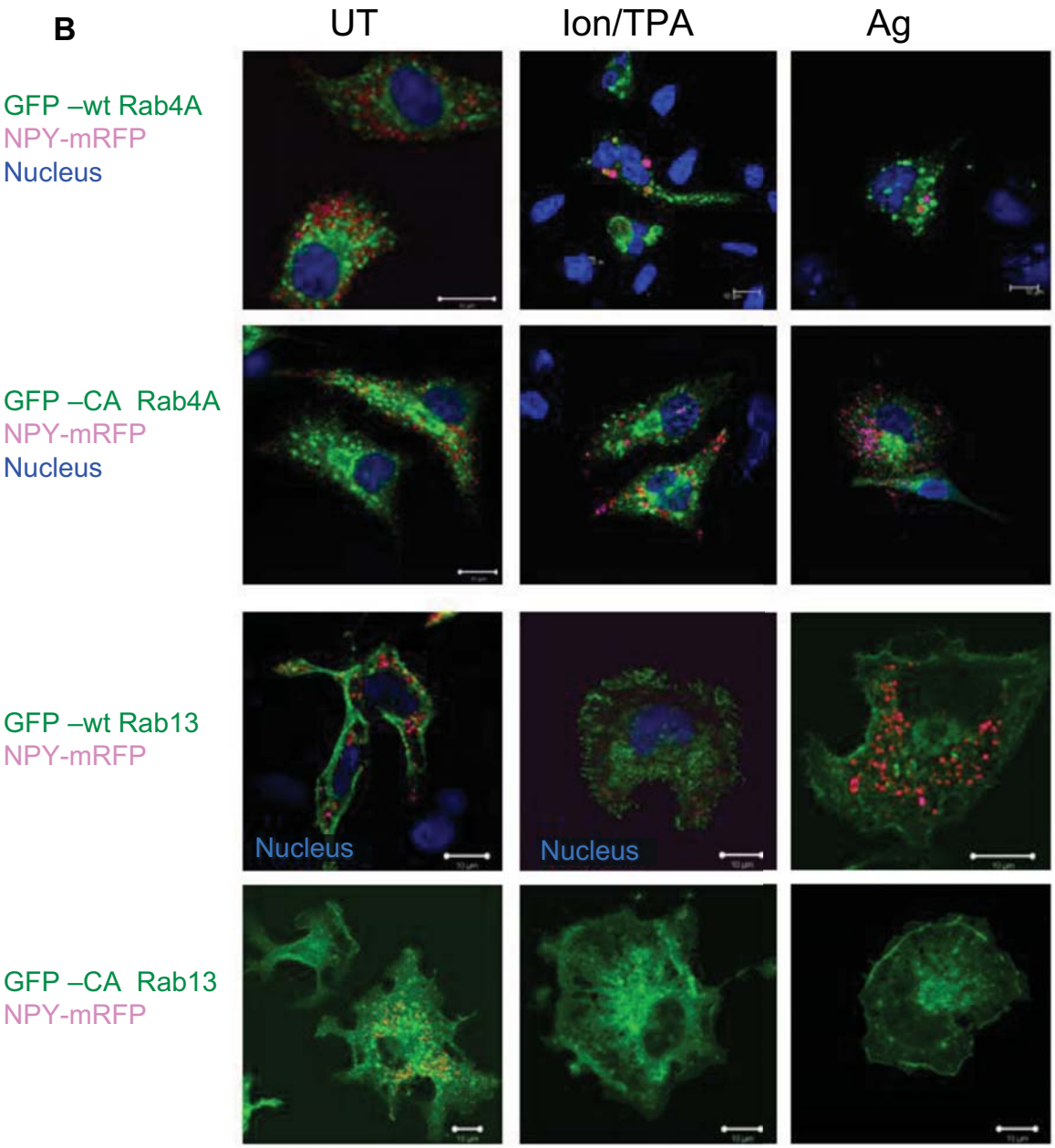

Supplemental Fig. S1B

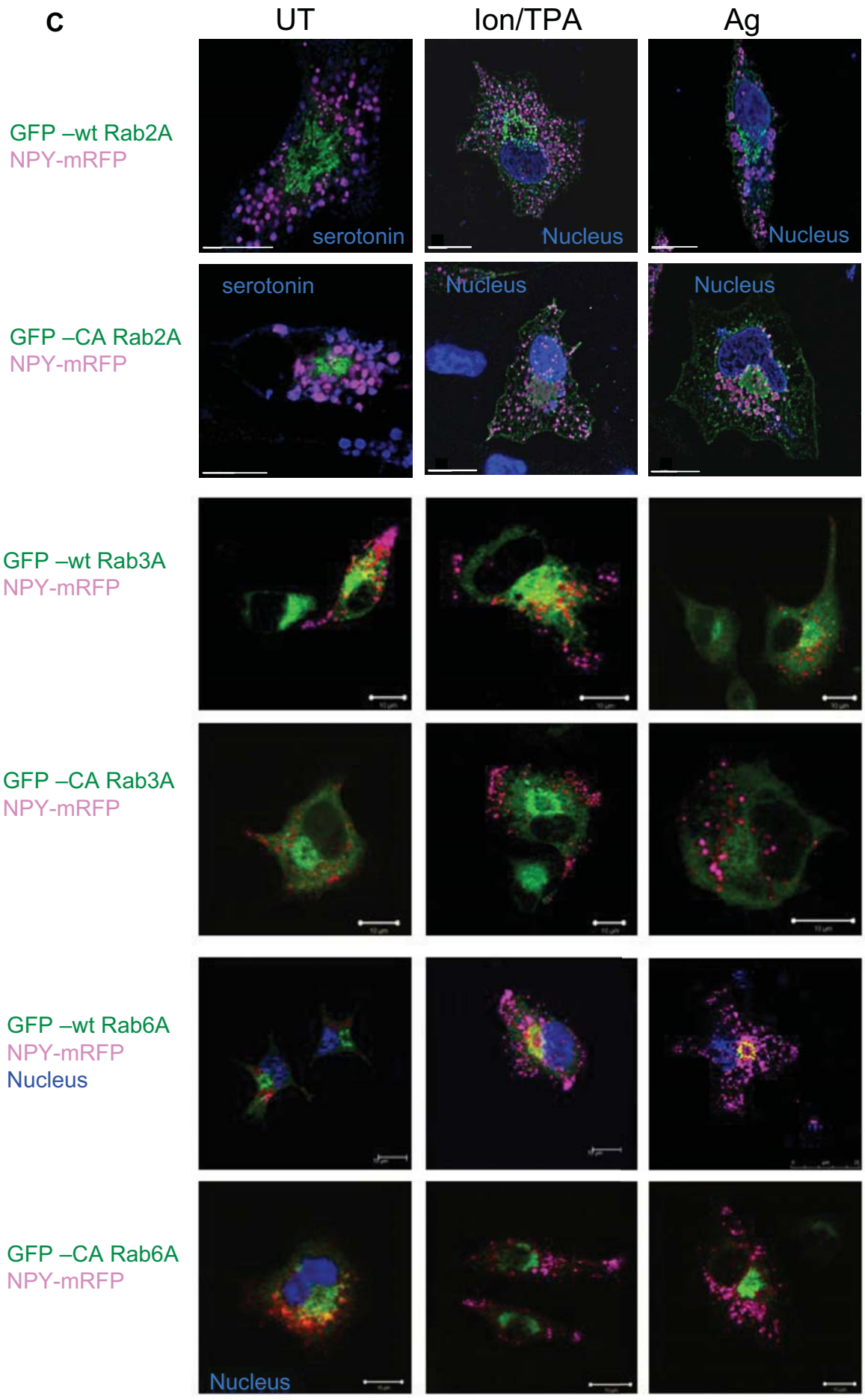

Supplemental Fig. S1C

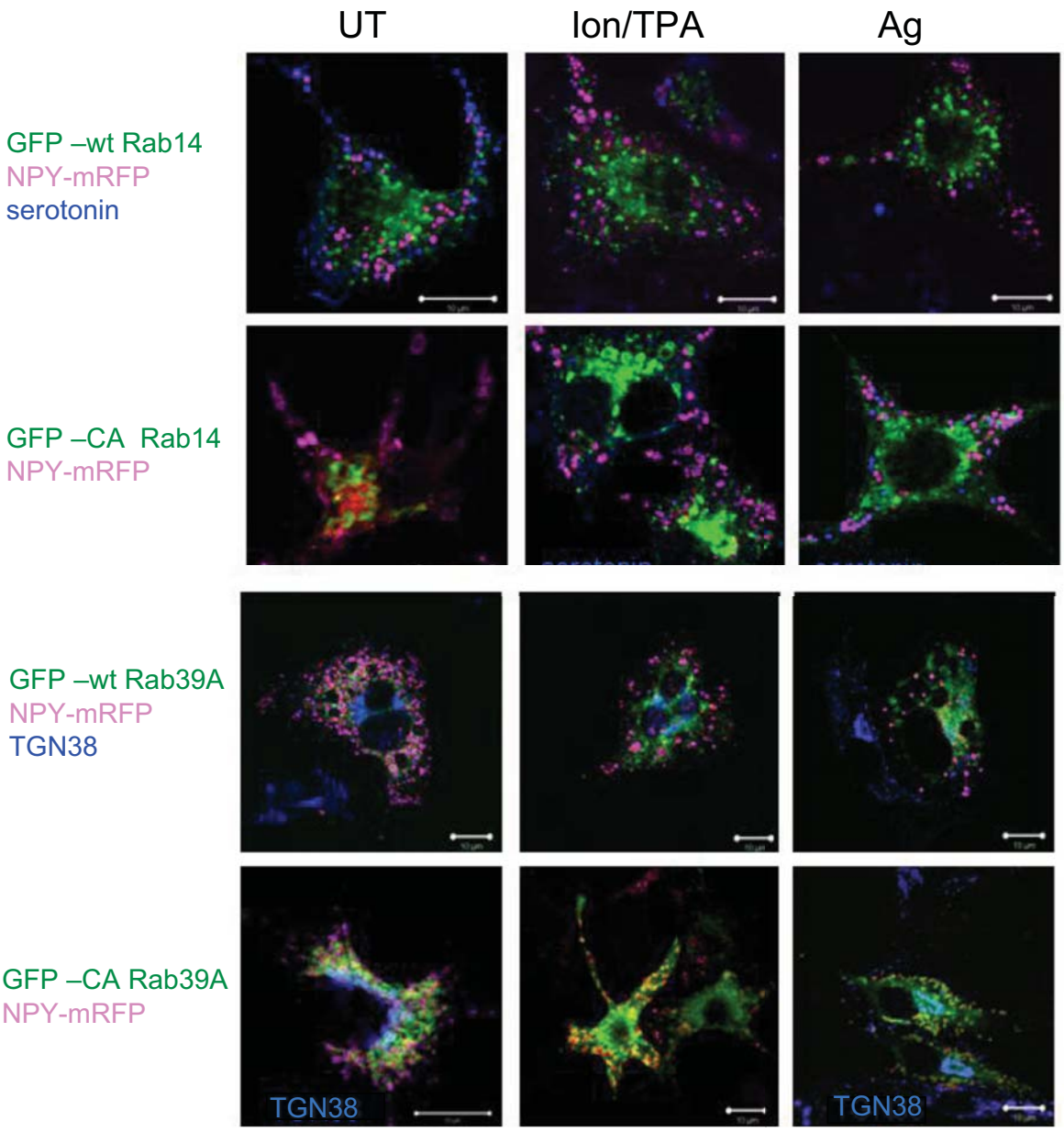

Supplemental Fig. S1C, continued

	Mean GFP fluorescence
GFP-wt Rab27A	102.17
GFP-CA Rab27A	73.66
GFP-wt Rab42	118.91
GFP-CA Rab42	162.27

Non transfected cells

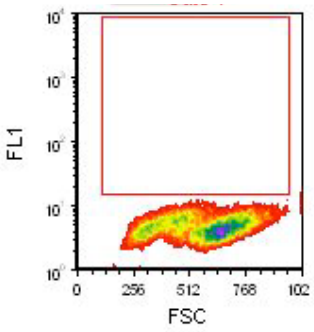

GFP-wt Rab27A

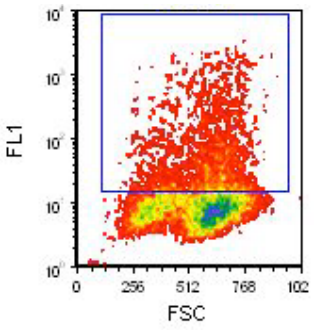

GFP-CA Rab27A

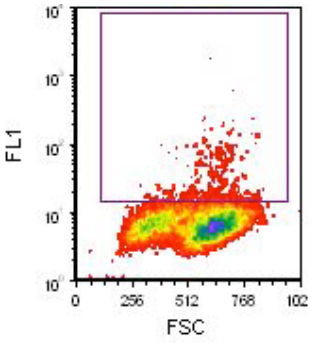

GFP-wt Rab42

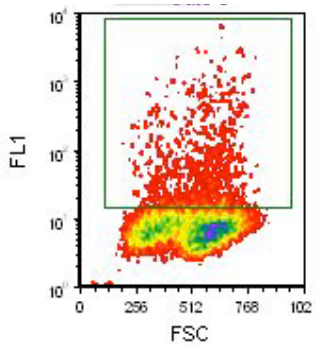

GFP-CA Rab42

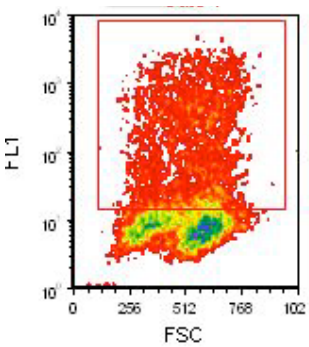

Supplemental Fig. S2

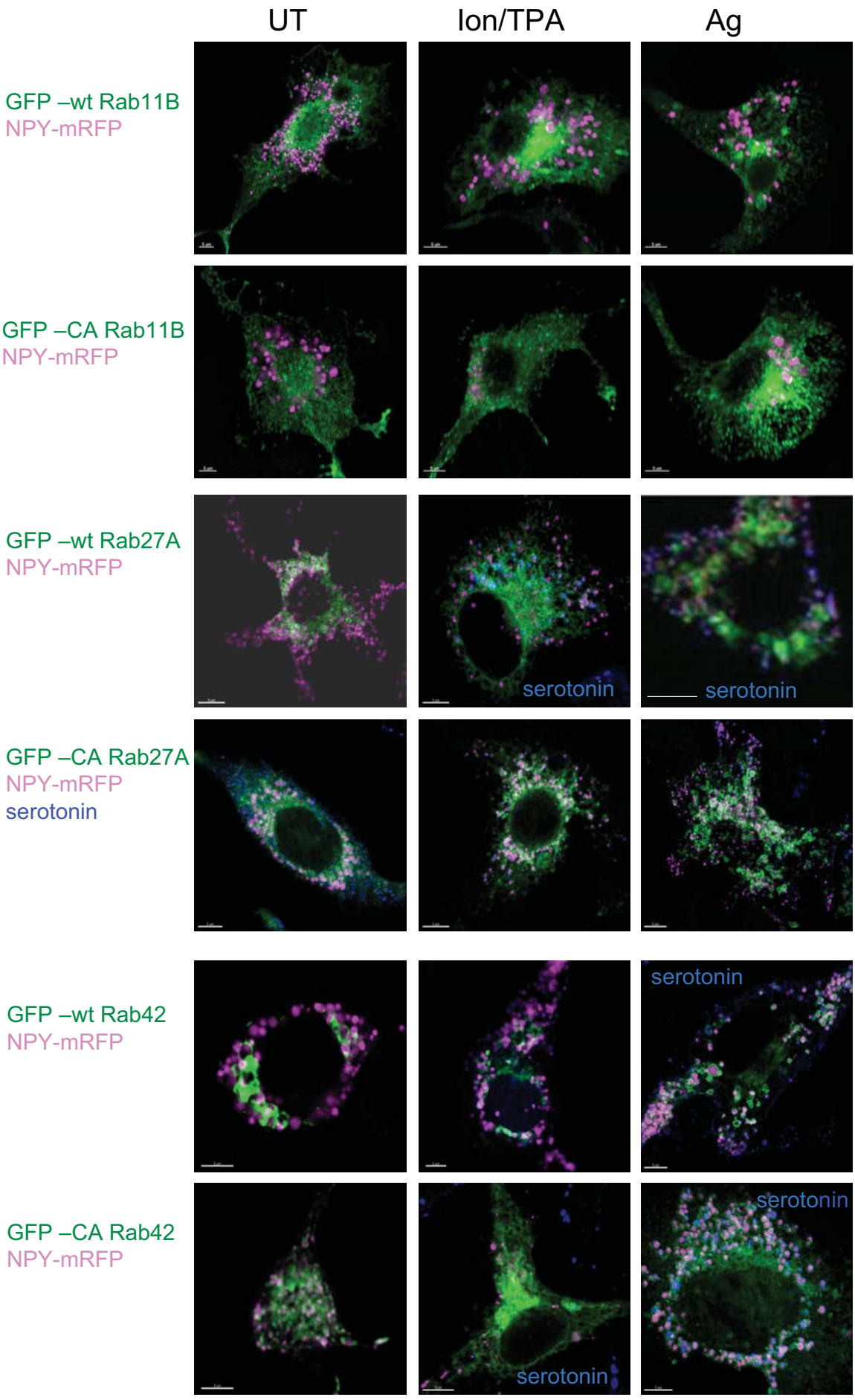

Supplemental Fig. S3

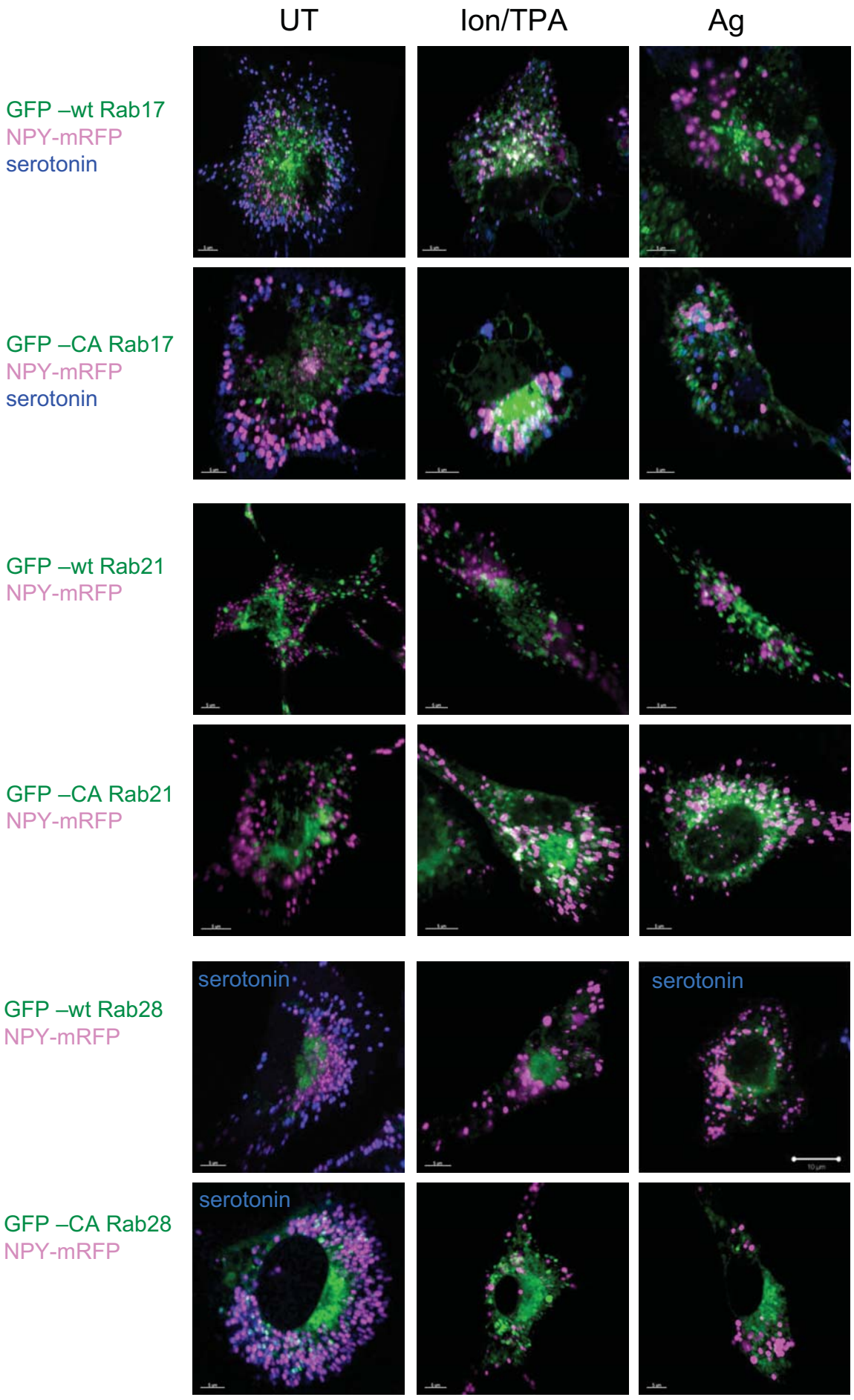

Supplemental Fig. S3, continued

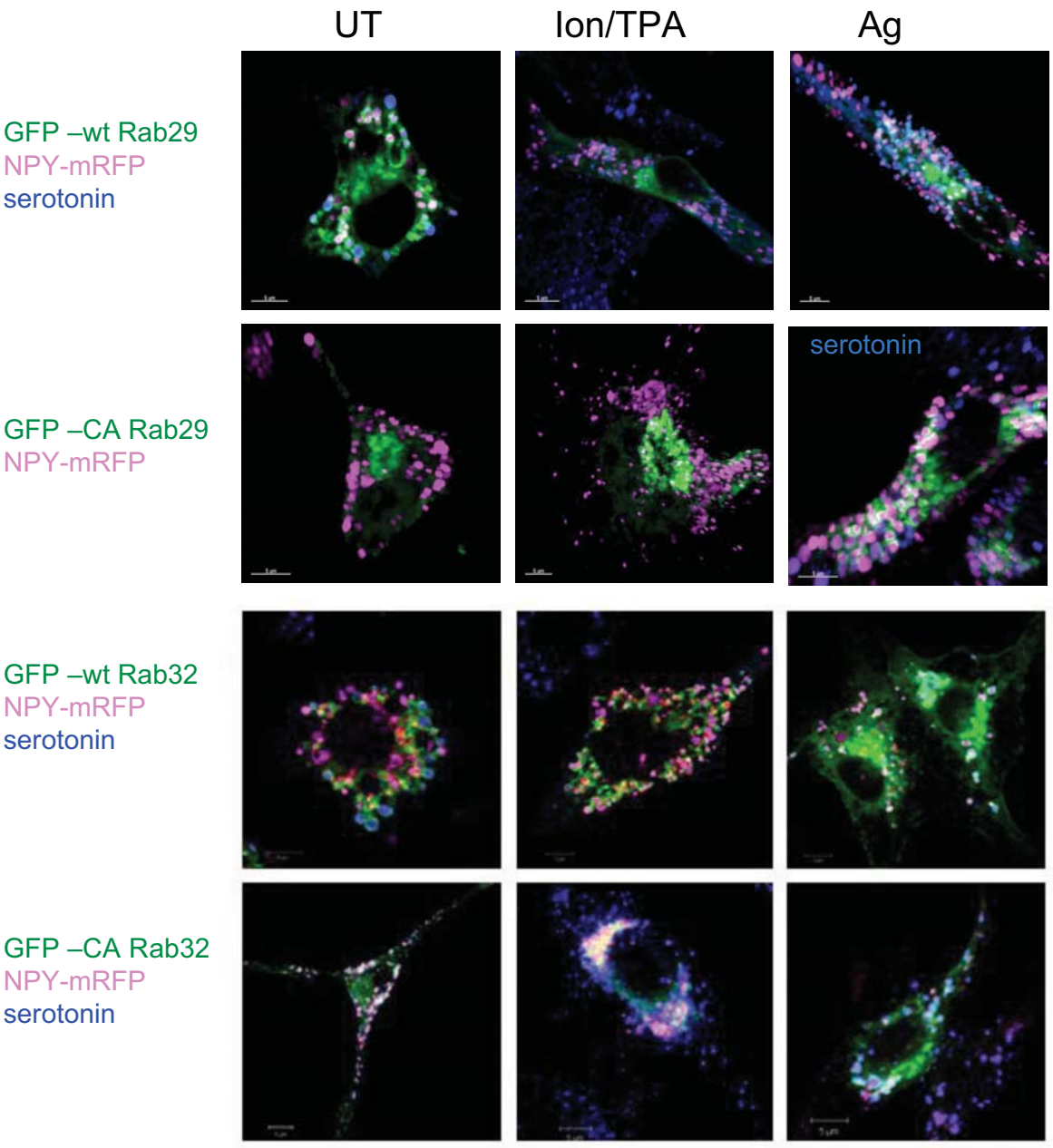

Supplemental Fig. S3, continued

Supplemental Table I: Expression profile of Rab GTPases in RBL cells

Rab GTPase	mRNA expression
Rab1A	V
Rab1B	V
Rab2A	V
Rab2B	V
Rab3A	V
Rab3B	V
Rab3C	V
Rab3D	V
Rab4A	V
Rab4B	V
Rab5A	V
Rab5B	V
Rab5C	V
Rab6A	V
Rab6B	V
Rab6C	V
Rab7	V
Rab8A	V
Rab8B	V
Rab9A	V
Rab9B	V
Rab10	V
Rab11A	V
Rab11B	V
Rab12	V
Rab13	V
Rab14	V
Rab15	V
Rab17	V
Rab18	V
Rab19	V
Rab20	V
Rab21	V
Rab22A	V
Rab23	V
Rab24	V
Rab25	V
Rab26	V
Rab27A	V
Rab27B	V
Rab28	V
Rab29/ Rab7L	V
Rab30	V
Rab31	V
Rab32	V
Rab33A	V
Rab33B	V
Rab34	V
Rab35	V
Rab36	V
Rab37	V
Rab38	V
Rab39A	V
Rab40B	V
Rab40C	V
Rab41	(-)
Rab42/ Rab7B	V
Rab43	V